Journal of Drug Delivery Science and Technology 114 (2025) 107459

Contents lists available at ScienceDirect

Journal of Drug Delivery Science and Technology

journal homepage: www.elsevier.com/locate/jddst

Harnessing Argonaute 2 as an innovative delivery system for siRNA in glioblastoma treatment

A. Rinaldi [a,b], E. Kluczka [a], M. Louis Fathy Nazir [a], M. Barbotin [a], C. Roy [a,e], L. Basset [a,c], S. Avril [a], S. Anthiya [a], G. Tosi [b], C. Jérôme [d], F. Boury [a], A. Rousseau [a,c], E. Garcion [a,e,f,1,*], F. Dumas [a,1,*]

[a] Université d' Angers, Inserm U1307, CNRS U6075, Nantes Université, CRCI2NA, Angers, France
[b] Università degli Studi di Modena e Reggio Emilia, Modena, Italy
[c] Department of Pathology, University Hospital of Angers, Angers, France
[d] Center for Education and Research on Macromolecules (CERM), Université de Liège, Liège, Belgium
[e] PRIMEX (Plateforme de Radiobiologie et d'Imageries Expérimentales), SFR, Université d'Angers, 4208, Angers, France
[f] PACEM (Plateforme d'Analyse Cellulaire et Moléculaire), SFR, 4208, Université d'Angers, Angers, France

A B S T R A C T

RNA interference via small interfering RNA (siRNA) offers promising potential for treating glioblastoma (GB), the most common and aggressive primary brain tumor. While local siRNA delivery could bypass the blood-brain barrier and achieve high drug concentrations, challenges remain in developing effective delivery systems that ensure siRNA stability, efficient cellular uptake, endolysosomal escape, and long-term brain availability. The Argonaute-2 (Ago2) protein, a core component of the RNA interference machinery, naturally binds siRNA and protects it from degradation. Ago2 is also found in biological fluids, such as blood, and in extracellular vesicles, including exosomes and microvesicles, making it a potential natural vector for siRNA delivery.

This study explores Ago2 as a natural vector for siRNA in nanoparticle-based delivery systems to enhance siRNA transport and gene silencing in GB. Neutral polymeric siRNA/Ago2-loaded nanoparticles (NPs), around 300 nm in size, were formulated with high encapsulation efficiencies (85.1 % for protein and 57.5 % for siRNA). In vitro testing in U87MG GB cells stably expressing luciferase (U87MG Bml1) showed that, in contrast to free siRNA/Ago2 complexes, siRNA/Ago2-loaded NPs effectively reduced luciferase expression compared to scramble siRNA formulations, with no significant cytotoxicity at 48 h. Interestingly, the introduction of exogenous Ago2 into cells unexpectedly upregulated luciferase expression, suggesting that Ago2 may also influence global gene expression beyond its role in siRNA-mediated silencing.

These findings highlight the potential of siRNA/Ago2-loaded NPs for local siRNA delivery in GB and suggest that Ago2 could play a broader regulatory role in gene expression, in addition to enhancing siRNA activity. Further investigation is needed to explore Ago2's impact on gene regulation and its potential as a therapeutic tool in GB treatment, particularly in combination with biocompatible hydrogels for sustained delivery.

1. Introduction

Glioblastoma (GB) is the most frequent and aggressive tumor of the Central Nervous System. Despite a combined approach based on surgery, radiotherapy, and chemotherapy with temozolomide, GB is still characterized by a very low median survival (12–18 months) and a high rate of tumor recurrences (>90 %) [1,2]. A significant advancement in recent decades is the antimitotic treatment using low-intensity alternating electric fields, known as Tumor Treating Fields (TTF, Optune®). While it extends survival by up to 21 months, it remains uncomfortable for patients and lacks curative potential [3]. Major obstacles to developing effective therapies include treatment resistance phenomena, tumor heterogenicity, the blood-brain barrier (BBB) that hampers the efficient brain accumulation of drugs, and numerous genetic and molecular alterations responsible for tumor growth and progression [4,5].

RNA interference (RNAi) is a potent biological mechanism that negatively regulates the expression of single or multiple genes into cells. RNAi molecules, including microRNAs and small interfering RNAs (siRNAs), have recently emerged as ideal therapeutic tools for GB [6]. siRNA nucleic acids work by entering the cell and specifically binding to its complementary messenger RNA (mRNA). This binding triggers the degradation of the targeted mRNA, preventing the synthesis of the corresponding protein [7]. In the context of GB, siRNA can be designed to silence genes that sustain tumor growth, survival, and

* Corresponding authors. Université d' Angers, Inserm U1307, CNRS U6075, Nantes Université, CRCI2NA, Angers, France.
E-mail addresses: arianna.rinaldi@unimore.it (A. Rinaldi), emmanuel.garcion@univ-angers.fr (E. Garcion), florence.dumas@univ-angers.fr (F. Dumas).
[1] Equivalent contribution

https://doi.org/10.1016/j.jddst.2025.107459
Received 18 February 2025; Received in revised form 22 August 2025; Accepted 26 August 2025
Available online 4 September 2025

chemoresistance [8]. Local delivery of siRNA into the brain represents a promising strategy to ensure high siRNA concentrations at the target site by circumventing the BBB [9]. With surgery being the standard of care for most GB patients, there is the possibility to exploit the tumor resection cavity for local drug administration near the tumor site post-surgery. However, even when the drug is administered locally, a drug delivery system is essential to shield siRNA from endonuclease degradation, facilitate its uptake into cells, and ensure it can escape the endolysosomal compartment and function effectively within cells. [10]. Nanoparticles (NPs), including liposomes, polymeric NPs, polymer-lipid hybrid NPs, dendrimers, and polymeric micelles, have provided the opportunity for effective siRNA delivery [11–14]. They are usually formulated with cationic polymers or lipids ensuring effective siRNA binding onto the surface or encapsulation into NP core by electrostatic interactions with the anionic siRNA [15–18]. Alternatively, anionic polymers such as Poly Lactic-co-Glycolic Acid (PLGA) are used, where siRNA is loaded into the NP core after pre-complexation with polycationic molecules such as Polyethyleneimine [19,20]. However, synthetic biomaterials usually show low biocompatibility and toxicity, especially polycationic ones, while natural ones generally ensure low transfection efficacy [21].

To address these challenges, a novel siRNA delivery strategy has been developed using a "biomimicking approach" [22,23], which draws inspiration from the natural mechanisms of RNA trafficking into cells. Most of the natural RNA transport processes have been reported to be protein-associated or protein-mediated [21]. Thus, natural RNA-carrier proteins as delivery vectors for siRNA may be promising in terms of biophysical and biochemical properties, presenting interesting features that cannot yet be reproduced by rational design, such as low toxicity, efficient endolysosomal escape, and high biocompatibility [24].

Ago2 protein is a crucial factor for the formation of RNA-induced silencing complex (RISC), the multiprotein complex that miRNA and siRNA join into cells to mediate the RNAi mechanisms [25]. In the RISC, the guide strand of an RNAi molecule interacts with the complementary strand of target mRNA, followed by the Ago-2-mediated mRNA degradation and the suppression of the translation process [7]. Ago2 (97 kDa) can be extrinsically loaded with a required siRNA without the need for other protein partners, and the rigid conformation of the protein-nucleic acid complex makes it resistant to protease attack [26,27]. Interestingly, 90 % of extracellular miRNAs internalized into cells for natural RNAi mechanisms have been estimated to be Ago2-bound. Abundant microRNAs are found in the bloodstream, associated either with extracellular vesicles (EVs) [28], lipoproteins [29], or circulating free Ago proteins [30], potentially serving endocrine signaling functions [31]. The association of RNAi with Ago2 has already been shown to increase miRNA uptake in human endothelial cells and glioma endothelium [32]. Moreover, the transmembrane protein Neuropilin-1 (nrp-1) has been identified as a receptor for extracellular transport of Ago2. Since nrp-1 is broadly expressed in endothelial cells and GB cells such as the U87MG cell line, it could play a major role in the cell internalization of Ago2 [33]. All this evidence suggests that siRNA/Ago2 complexes may be used as a potent, long-lasting delivery system for siRNA. Recent studies support this rationale; for instance, the use of miRNA/Ago2 complex as an extrinsic carrier for systemic miRNA delivery has been patented by Galas et al., in 2019 (patent #20190367918, 2019) to improve miRNA uptake in human endothelial cells. In another study, Li et al. demonstrated that preassembling siRNA with Ago2, followed by packaging with commercial transfection reagents or structurally defined polycations, enhanced siRNA-mediated gene silencing in cell lines and a melanoma mouse model [34]. In the case of siRNA, the affinity for Ago2 for siRNA has been described as a long-lasting binding, with a complex half-life of days or weeks *in vitro*. However, it has still not been proven whether Ago2 can cross or not the BBB and efficiently deliver the drug in the context of a brain tumor [35]. Thus, encapsulating Ago2 with siRNA and loco-regionally delivering it to GB might be a pertinent strategy. This project aims to develop a siRNA nanodrug using Ago2 as a protein-mediated siRNA vehicle for locoregional GB therapy. To this aim, siRNA/Ago2 complexes were developed and tested *in vitro*, either free or encapsulated into NPs formulated with Polyethylene Glycol-Poly Lactic-co-Glycolic Acid (PEG-PLGA) and PLGA with capped carboxylic acid terminals (PLGA-COOR) polymers. PLGA-based NPs have been previously studied by our group for the delivery of therapeutic proteins, demonstrating the possibility of achieving long-term protein release using NP-incorporating scaffold systems for GB locoregional therapy [36]. This technology may be extended to the delivery of siRNA/Ago2 complexes, to achieve sustained release of siRNA and protect it into the core of NPs. In this study, the pre-complexation of anionic siRNA with the positive charges of Ago2 may play a key role in promoting the encapsulation of siRNA into NPs, as a safer alternative to polycationic materials commonly used to achieve this purpose (e.g. polyamines) [19]. In this work, siRNA/Ago2 NPs were formulated using a three-step process. First, a complex between a model siRNA (siRNA-NC) and Ago2 protein was formed. This complex was then precipitated by the addition of water-miscible organic solvent [37], to preserve the protein structural integrity and enhance protein encapsulation into polymeric NPs [38]. The product was then loaded into NPs made of PEG-PLGA and PLGA-COOR NPs using a phase-separation method [39,40]. During this process, the correct complexation of siRNA and Ago2 was evaluated, together with protein precipitation and encapsulation efficiency of both siRNA and Ago2. The formulated nanoparticle stability was assessed before and after freeze-drying, as well as the protein release in a medium experiment. The functionality and efficiency of the siRNA/Ago2 complex, either free or in the form of siRNA/Ago2 NPs, was verified by characterizing its luciferase gene silencing activity *in vitro* on a luciferase gene expressing GB cell line (U87MG Bml1).

2. Materials and methods

2.1. Materials

Ester-capped PLGA (PLGA-COOR) (Mn = 5.5 kDa, PDI 2.0) and PEG-PLGA copolymer (MnPEG = 5 kDa, MnPLGA = 25.7 kDa, PDI 2.1) were synthesized using a ring-opening polymerization method as previously described [37]. U87MG (Bmi1-3′UTR) luciferase-expressing human glioblastoma cell line (HTB-14TM) was obtained from the American Type Culture Collection (Manassas, United States) and modified at the Vector Production Center, Inserm U1089, Atlantic Gene Therapies facility in Nantes (FRANCE). Firefly luciferase custom-designed siRNA (Luc-siRNA) and MISSION® siRNA Universal Negative Control #1 (Sigma: SIC001) (C-siRNA) were both obtained from Sigma®. Recombinant human Argonaute 2 EIF2C2 protein (Cat# 11079-H07B) was obtained from Sino Biological (Beijing, China). Argonaute 2 ELISA kit from Bioassay Technology Laboratory (Shanghai, China), and D-Luciferin sodium salt were purchased from Abcam (Amsterdam, Netherlands). Glycofurol (tetrahydrofurfuryl alcohol polyethyleneglycol ether), isosorbide dimethyl ether (DMI), sodium chloride (NaCl), poloxamer 188 (Lutrol® F68), glycine, 37 % hydrochloric acid (HCl), sodium hydroxide (NaOH), tris(hydroxymethyl)aminomethane base (Tris, Trizma®), resazurin sodium salt, HEPES sodium salt, ethylenediaminetetraacetic acid disodium salt (EDTA), DL-Dithiothreitol (DTT), glycerol, puromycin, antibiotic-antimycotic solution and Dulbecco's Modified Eagle's Medium (DMEM, Gibco®) were obtained from Sigma-Aldrich® (Saint Quentin Fallavier, France). Blue/Orange Loading Dye, 6X (0.4 % orange G, 0.03 % bromophenol blue, 0.03 % xylene cyanol FF, 15 % Ficoll® 400, 10 mM Tris-HCl pH 7.5 and 50 mM EDTA pH 8.0) was purchased from Promega Corporation (Madison, Wisconsin, USA). Hydroxypropyl-β-cyclodextrin (HPBCD, Kleptose®) was purchaised from Roquette (Lestrem, France), Dulbecco's phosphate-buffered saline (Biowhittaker®) from Lonza (Verviers, Belgium), and LipofectamineTM RNAiMAX reagent from Thermo Fisher Scientific (Villebon sur Yvette, France). Ultrapure water was dispensed from a Milli-Q® Advantage A10 system (Millipore, Paris, France), or

RNase-free water (Qiagen, Hilden, Allemagne) when specified, was used in all experiments.

2.2. Preparation and qualitative assessment of siRNA/Ago2 complexes

2.2.1. Preparation of siRNA/Ago2 complexes

To form a complex of siRNA with Ago2, a complexation buffer was prepared containing 0.01 M HEPES, 150 mM NaCl, 3 mM EDTA, 1 mM DTT, and 10 % glycerol in RNAse-free water was first prepared. Next, 0.02 nmol control siRNA (siRNA-NC) was mixed with varying volumes of an Ago2 aqueous solution (0.5 mg/mL) to achieve various Ago2: siRNA molar ratios (0.03:1; 0.06:1; 0.12:1; 0.25:1; 0.5:1; 1:1, and 2:1). The complexation buffer was added to each sample to reach a final volume of 10 μL, and a final siRNA concentration of 2 μM. The mixture was left to incubate at room temperature for 30 min. For *in vitro* studies, siRNA/Ago2 complexes were prepared at the Ago2: siRNA molar ratio of 1:1 using both siRNA-NC and Firefly luciferase siRNA (siRNA-Luc) targeting luciferase mRNA sequence.

2.2.2. Qualitative assessment of siRNA/Ago2 complex formation

To qualitatively assess the formation of complexes between siRNA and Ago2, an Electrophoretic Mobility Shift assay (EMSA) was performed. Complexes were prepared as previously described by tripling the quantity of Ago2, siRNA, and the volume of buffer to obtain 30 μL of the sample. Complexes were then mixed with Blue/Orange Loading Dye, 6X, and then loaded onto a 3 % w/v agarose gel stained with ethidium bromide (0.5 μg/mL). Electrophoresis was conducted at 100 V for 45 min in TBE buffer 1X using a horizontal electrophoresis apparatus (Elettrofor Horizontal Electrophoresis unit; MOD. OA-160; Elettrofor s. a.s., Borsea, Italy). The migration of siRNA was recorded by a gel imager (Amersham Imager AI680, GE Healthcare, ChicAgo, USA). The formation of the siRNA/Ago2 complex was qualitatively assessed by observing the shift of the less mobile complex on the gel, compared to the mobility of a control spot obtained by running free siRNA in the absence of protein.

2.3. Preparation of Ago2 and siRNA/Ago2 precipitates (Ago2 NPR and siRNA/Ago2 NPR)

To precipitate siRNA/Ago2 complexes or Ago2 as a control, a technique adapted from Giteau et al. was employed [38]. Firstly, a buffer solution named P188-NaCl-Tris HCl was prepared. To obtain it, a 0.2 M Tris-HCl aqueous solution was adjusted to pH 9.75, and NaCl was added until a final concentration of 0.45 M, 0.9 M, or 1.3 M NaCl was achieved. Then, P188 was dissolved in its respective NaCl-Tris-HCl solutions up to a 0.06 % (w/v) concentration. After the buffer solution was prepared, 10 μL of Ago2 alone or siRNA/Ago2 complexes were added to 67 μL of the P188-NaCl-Tris HCl solution to create an aqueous phase. The 77 μL aqueous phase was added to 123 μL glycofurol (pH 5.5), the mixture was stirred, and then it was incubated at 4 °C for 30 min. This step was conducted by testing different stirring conditions (after 10 times pipetting, without any stirring, or after homogenizing at 10 min with a 3-speed vortex for 10 s). The effect of the stirring condition on the precipitate size and morphology was analyzed to optimize the precipitation process. Mixing the Tris-HCl buffer solution with glycofurol resulted in a final precipitate suspension at pH 9.3, which is equivalent to the protein isoelectric point and helps enhance the precipitation efficiency (PE). To evaluate the PE, the suspension of protein precipitates was centrifuged at 14,000g for 30 min. The supernatant was then removed, and the pelleted precipitates were dissolved in 1 mL of 0.05 M Tris-HCl buffer solution and diluted for further quantification. The concentration of Ago2 in the suspension was determined using an indirect sandwich ELISA as described in section 2.5.8. (*Ago2 quantification*), to determine the mass of Ago2 recovered from the precipitate. PE was calculated using Eq. (1).

$$\textit{Precipitation Efficiency}\ (PE, \%) = \frac{\text{mass (μg) of protein recovered from the precipiate}}{\text{Initial mass (μg)of protein added to the precipitate x100}} \quad (1)$$

PE was determined on precipitates prepared at different salt concentrations (0.45 M, 0.9 M, or 1.3 M NaCl) in the P188-NaCl-Tris HCl solution, to select the optimal concentration ensuring the highest PE value.

2.4. Preparation of Ago2-loaded and siRNA/Ago2-loaded nanoparticles

NPs loaded with Ago2 only (Ago2 NPs) or with siRNA/Ago2 complex (siRNA/Ago2 NPs) were prepared by adapting a protocol from Mansor et al. [37]. Briefly, 100 μL of Ago2 or siRNA/Ago2 precipitates were mixed with 200 μL of a 12 % w/v PEG-PLGA solution and 100 μL of a 12 % w/v PLGA-COOR solution, obtained by dissolving the polymers in isosorbide dimethyl ether. Control unloaded NPs and NPs loaded with siRNA but not Ago2 (siRNA-NPs) were prepared by replacing the protein precipitates with an equal volume of glycofurol or siRNA dissolved in glycofurol, respectively. Then, nanoprecipitates were formed by adding 200 μL of a 0.05 M glycine-sodium hydroxide buffer aqueous solution under constant magnetic stirring at 1300 rpm. The pH of the glycine solution was set to the protein isoelectric point (pI 9.3) to enhance encapsulation efficiency. After 1 min, another 500 μL Gly-NaOH was added dropwise, and this step was repeated three times by waiting 30 s between each step. Subsequently, the formed NPs were washed with water up to 30 mL to remove any residual solvent out of the NPs. After 1 h incubation at room temperature, the NP suspension was centrifuged at 8,500g for 30 min at 25 °C. The supernatant was collected and stored at −20 °C, while the NP pellet was re-suspended in 250 μL water and used for further analysis.

2.5. Nanoparticle characterization

2.5.1. Size, size distribution and zeta-potential

The size, Polydispersity Index (PDI), and Z-Potential of nanoprecipitates and NPs were measured by diluting formulations up to 0.01 mg/ml. Samples were analyzed by a Zetasizer Nano ZS (Malvern Panalytical Ltd., Malvern, UK) at 25 °C by Dynamic Light Scattering technique. All measurements were performed at least in triplicate from three different formulations.

2.5.2. Weight yield (%)

To determine the weight yield of NPs, an aliquot of NP suspension was placed in a pre-weighted Eppendorf® tube and then freeze-dried using a Lyovax® GT freeze-dryer (Steris, Bordeaux, France) pre-cooled at −35 °C for 2 h. The weight yield was calculated using Eq. (2).

$$\textit{Weight Yield}\ (\%) = \frac{\textit{mass (mg) of solid recovered after freeze} - \textit{drying}}{\textit{initial mass (mg)of polymer}}\ x\ 100 \quad (2)$$

2.5.3. Nanoparticle stability to freeze-drying

An aliquot of purified NPs was mixed with an aqueous solution of 2-Hydroxylpropyl-beta-cyclodextrin (HPBCD) or sucrose in an Eppendorf® tube, to reach a cryoprotectant final concentration of 5 % (w/v) in the tube and a final nanoparticle concentration of 18 mg/mL. The mixture was then frozen in liquid nitrogen and lyophilized at −20 °C and 0.3 mbar overnight. A cryoprotectant-free NP sample was used as a control. After 24-h storage, freeze-dried NPs were re-suspended in the same initial volume of water as the one after NP purification. Then, the size and size distribution of NPs were measured before and after freeze-drying on NP suspension diluted up to 100 μg/mL. NPs were considered to be stable after the freeze-drying process if the ratio of final to initial size (Sf/Si) and polydispersity index (PDIf/PDIi) is close to 1 [37].

2.5.4. Morphology

The morphology of precipitates and precipitate-loaded NPs was evaluated by Transmission Electron Microscopy (TEM, JEM 1400, JEOL, Paris, France). Briefly, 2 μL of undiluted protein precipitates were deposited on a carbon-coated copper grid and the organic solvent (glycofurol) of the sample was washed out by dipping for a few seconds the grid on the sample side in a water droplet put on a paraffin layer. The excess water was absorbed using Kimtech® precision wipes and the grid was put back on a paraffin-covered Petri dish. The sample was let to dry overnight under a fume cupboard at room temperature. A TEM holder with a sloping plane was used to verify the surface morphology of the samples. For the NPs, samples were prepared via the same procedure as the precipitates, except that the NP suspension was first diluted (200 μg/mL) in 0.01 M NaCl solution, and samples were let dry for 4h before TEM analysis. NPs were also analyzed by Scanning Electron Microscopy (SEM, JSM 6310F, JEOL, Paris, France). Briefly, water-diluted NP suspension (200 μg/mL) was added on a glass slide and left to dry overnight at R.T. The sample was coated with a gold layer of 5 nm thickness before observation.

2.5.5. Ago2 encapsulation efficiency

To evaluate the Ago2 encapsulation efficiency (EE), the supernatant obtained from Ago2 NPs or siRNA/Ago2 NPs during the purification step by centrifugation was collected as described in section 2.4. The same procedure was applied to unloaded NPs, used as control. The EE was calculated using Eq. (3).

$$EE\ (\%) = 100 - \left(\frac{\text{mass of protein recovered from the supernatant}}{\text{initial mass of protein used to formulate NPs}} x\ 100\right) \quad (3)$$

The mass of protein recovered from the supernatant was determined using an indirect sandwich ELISA as described in section 2.5.8. (*Ago2 quantification*). To simulate the 100 % presence of the protein in the supernatant, an amount of protein precipitate equivalent to the initial mass used to formulate NPs was diluted in 30 mL of water (which is equivalent to the volume of supernatant collected) and quantified as well.

2.5.6. siRNA encapsulation efficiency

The 250 μL of purified siRNA/Ago2 NP suspension was mixed with 750 μL acetonitrile (ACN) and vortexed for three cycles to solubilize NPs. Then, 100 μL of the mixture was transferred in a 96-well plate, and the amount of encapsulated siRNA was quantified by RiboGreen® Assay following the manufacturer's protocol. i) Unloaded NPs, ii) Ago2 NPs, iii) siRNA NPs (formulated without Ago2) undergoing the same procedure as siRNA/Ago2 NPs, and iv) ACN only were used as controls to perform the test. The EE was calculated using Eq. (4).

$$EE\ (\%) = \left(\frac{\text{mass (μg) of recovered siRNA}}{\text{initial mass (μg) of siRNA used to formulate NPs}}\right) x\ 100 \quad (4)$$

2.5.7. Ago2 release studies

After formulating NPs following the procedure previously described, NPs were centrifuged to collect them. The Ago2-loaded NPs pellet was resuspended in 2 mL Dulbecco's phosphate-buffered saline (PBS) medium (pH = 7.4) and incubated at 37 °C. At pre-defined time intervals (0 h, 24 h, 48h, 72h, and 96h), an aliquot of the release medium was collected, and an ELISA was performed on appropriately diluted samples to quantify Ago2 released from NPs with time.

The percentage of released protein was calculated following Eq. (5).

$$\text{Release drug} = \left(\frac{\text{mass of released protein}}{\text{initial mass of protein}}\right) x\ 100 \quad (5)$$

Sampling was performed in triplicate. To normalize the percentage of protein release to the total amount of loaded protein (100 %), NPs were dissolved in 1 mL of dimethyl sulfoxide for 1 h, 3 mL of 0.01 M HCl was added to liberate the protein from the polymeric NPs, and the released Ago2 was quantified by ELISA assay as well.

2.5.8. Ago2 quantification

Ago2 protein in precipitates and NP dispersions was quantified following a sandwich indirect ELISA method using the Human Protein Argonaute-2, EIF2C2 ELISA kit obtained from BT Lab®. Briefly, kit components were reconstituted using their respective diluent and following the kit procedure. Ago2 standard serial dilutions were prepared and deposited alongside the precipitates and NP supernatant samples on a 96-well plate pre-coated with an anti-Ago2 capture antibody. The biotinylated detection antibody anti-Ago2 was added to each well except for the standard, which already contained the antibody. Afterwards, streptavidin-HRP detection reagent was added to each well and the plate was left to incubate for 1h at 37 °C. After removing reagents and performing 5 washing steps with PBS, the two substrates were added to each well, and the plate was incubated in the dark at 37 °C for 10 min. After adding stop solution, wells absorbance was read using continuous dual measurement mode at 450 nm and 580 nm with the Thermo Labsystems Multiskan Ascent 354 Microplate Reader (Thermo Fisher Scientific, Villebon sur Yvette, France). Absorbance at 580 nm was subtracted from the 450 nm one to eliminate any interfering signal. Samples were obtained from formulations prepared in triplicate.

2.6. In vitro analysis

2.6.1. Cell line generation and culture

The human glioblastoma cell line U87MG modified to stably express the luciferase gene (U87MG (Bmi1-3′UTR)) was generated as previously described [41]. Cells were maintained in complete DMEM, composed of Dulbecco's Modified Eagle's Medium (DMEM, Sigma-Aldrich® Saint Quentin Fallavier, France) supplemented with 10 % heat-inactivated Fetal Bovine Serum (FBS, Roche Diagnostics, Mannheim, Germany) and 1 % antimycotic-antibiotic mix (Sigma-Aldrich®, Saint Quentin Fallavier, France) in a humidified 5 % CO_2 incubator at 37 °C.

2.6.2. Luciferase gene silencing and cell viability studies

U87MG (Bmi1-3′UTR) cells were seeded at a density of 5000 cells/well in a white μClear® 96 multiwell plate (Greiner Bio-one, Les Ulis, France). After 24 h, cells were treated with i) 20 nM free luciferase-specific siRNA (siRNA-Luc) or a negative control siRNA (siRNA-NC); ii) 20 nM free Ago2 protein; iii) siRNA/Ago2 complexes, by complexing the protein with both siRNA-NC and siRNA-FLuc, at an Ago2 equivalent concentration of 20 nM; iv) siRNA-Luc and siRNA-NC using Lipofectamine™ RNAiMAX transfection agent (Thermo Fisher Scientific, Villebon sur Yvette, France) as a positive control, at a siRNA: RNAiMax ratio prepared according to the manufacturer's protocol; v) NPs encapsulating precipitated Ago2 or vi) precipitated siRNA/Ago2 complexes (Ago2 NPs and siRNA/Ago2 NPs, respectively) to have 20 nM as final Ago2 concentration for each well; vii) unloaded NPs; viii) the medium

only. After 24 h incubation at 37 °C and 5 % CO2, the medium was replaced with 100 μL complete DMEM. After a total incubation time of 48 h, the medium was replaced with 100 μL per well of a solution 0.15 mg/mL of StayBrite™ D-Luciferin sodium salt (M.W. 302 g/L, Abcam, Amsterdam, Netherlands) in complete DMEM medium. The Luminescence signal per well was read within 15 min at 580 nm using CLARIOstar® Microplate Reader (BMG Labtech, Ortenberg, Germany) at 37 °C. A resazurin viability assay was then performed to normalize luciferase expression to the relative number of viable cells. Briefly, the D-Luciferin solution in each well was replaced with 100 μL of a solution of 44 μM of resazurin in a complete DMEM medium. After 1 h incubation at 37 °C, 5 % CO_2, the fluorescence intensity of each well was measured at 545 nm excitation and 600 nm emission. Each condition was performed at least in duplicate for each analysis, and each experiment was repeated in triplicate (n = 3). Luciferase expression normalized to the number of viable cells was calculated following Eq. (6).

$$Relative\ Luciferase\ Expression\ (RLE\%) = \frac{\left(\frac{ALU}{RCN}\right) per\ well}{\left(\frac{ALU}{RCN}\right) untreated\ cells}\ x\ 100 \quad (6)$$

ALU (Arbitrary Luminescence Unit) refers to the luminescence signal measured in each well. RCN (Relative Cell Number) corresponds to the percentage of viable cells for each well relative to non-treated cells, calculated using the following Eq. (7):

$$Relative\ Cell\ Number\ (RCN, \%) = \frac{fluorescence\ per\ well}{fluorescence\ from\ untreated\ cells}\ x\ 100 \quad (7)$$

2.7. Statistical analysis

Data are presented as the mean value ± standard deviation (SD) of at least three experiments (n ≥ 3). One-way ANOVA with post-Dunnet's multiple comparison test with a threshold P-value of 0.05 was used to investigate any significant difference between multiple groups of data. GraphPad Prism 6 software was used (GraphPad Holdings, San Diego, CA, USA). In the figures, * indicates P ≤ 0.05, ** indicates P ≤ 0.01, *** indicates P ≤ 0.001 and **** indicates P ≤ 0.0001.

3. Results and discussion

Although the role of Ago2 as a protein vector for RNAi remains unclear due to limited research, evidence indicates that Ago2-RNAi complex formation could stabilize and enhance RNAi delivery. This positions Ago2 as a promising RNAi vector candidate for RNAi-based therapies to improve siRNA delivery and gene silencing. In the context of locoregional GB therapy, we first explored whether Ago2 could function as a protein carrier for siRNAs to GB cells *per se* in the form of siRNA/Ago2 complexes. Still, we found that it does not naturally or trivially fulfill this role. Thus, leveraging Ago2's ability to stabilize siRNAs and form a minimal RISC-like complex *in vitro*, we sought to optimize its potential as a natural vector by incorporating it into a nanoparticle (NP) -based delivery system for enhanced therapeutic efficacy. To this aim, siRNA/Ago2 complexes were formed and tested *in vitro*, either in their free form or encapsulated within NPs.

3.1. Precipitation and encapsulation of Ago2 into PLGA-PEG/PLGA-COOR NPs to advance Ago2-based RNAi delivery strategies

To enhance Ago2-based RNAi delivery, an NP-based formulation was developed to deliver siRNA as siRNA/Ago2 complexes (siRNA/Ago2 NPs). NPs were obtained by a three-step formulation process. First, a complex between a model siRNA (siRNA-NC) and Ago2 protein was formed. This complex was then precipitated by adding a water-miscible organic solvent (glycofurol) before encapsulation into NPs [37]. Finally, the resulting nanoprecipitates were encapsulated into NPs based on PEG-PLGA and PLGA-COOR polymers using a phase-separation method [39,40]. Before studying the co-encapsulation of Ago2 and siRNA as a complex, an optimization of the Ago2 precipitation process and encapsulation into NPs was performed for formulations containing Ago2 only (Ago2 NPs). These steps are described in this section (3.1) and in section 3.2. Once the formulation parameters were optimized, they were used to formulate and characterize NPs loaded with siRNA/Ago2 (section 3.3).

3.1.1. Development of Ago2 nanoprecipitates

Protein precipitation before encapsulation into polymeric NPs is a critical step to preserve protein structural integrity, enhance encapsulation into NPs, and minimize protein adsorption onto the polymer [38]. Thus, Ago2 protein precipitates were first prepared by dissolving the protein in an aqueous solution of salt and a surfactant, followed by addition to an organic solvent under stirring. Sodium chloride (NaCl) salt was used to neutralize the charged protein and promote attractive hydrophobic interactions, while P188 surfactant was added to reduce protein adsorption to the hydrophobic PLGA during encapsulation [42]. Evidence suggests that protein precipitation is strongly influenced by stirring conditions and the type of salt used [43]. Therefore, to optimize this process, the effects of these variables on the size and morphology of Ago2 precipitates were studied.

The effect of stirring was evaluated by preparing three samples of Ago2 precipitates under different stirring conditions: vortexing for 10 s, no stirring, and gentle pipetting immediately before incubation on ice. The salt concentration was kept constant at 0.3 M NaCl.

Among these, vortexing produced the smallest precipitates (208 ± 23) and offered better reproducibility due to its experimenter-independent nature, making it the chosen method for subsequent steps (Fig. S1). The impact of NaCl concentration was then assessed by preparing precipitates with different concentrations (0.15 M, 0.3 M, and 0.45 M) and analyzing their size and morphology using TEM. TEM images were acquired using a sloping plane, to observe the three-dimensional structure of the precipitates. The size of the precipitate was significantly affected by the concentration of NaCl, with increased precipitate sizes at the lowest and the highest salt concentrations. The precipitate size was 370 ± 36 nm at 0.15 M NaCl, 273 ± 23 nm at 0.30 M NaCl, and 306 ± 30 nm at 0.45 M NaCl (Fig. 1a). By contrast, all samples exhibited a spherical morphology regardless of the salt concentration (Fig. 1b). In the absence of NaCl, no effective precipitation occurred, and no precipitates were observed. The size of these nanoprecipitates is crucial, as it may influence the size of loaded NPs and their cellular internalization pathway. To follow the literature-described clathrin-independent or clathrin-dependent endocytic mechanism, the size of NPs should not be higher than 500 nm [44,45]. Since the effect of salt concentration can also affect the correct protein precipitation [37], the Ago2 precipitation efficiency (PE) was evaluated using an indirect sandwich ELISA for the three NaCl concentrations (0.15, 0.3, and 0.45 M). The PE values were found to be 49 ± 4 %, 51 ± 5 %, and 52 ± 5 %, for the 0.15 M, 0.3 M, and 0.45 M of NaCl, respectively. Thus, Ago2 PE was found not to be affected by the salt concentration (Fig. 1c). By contrast, the absence of salt prevented the salting-out process as previously described and thus limited to effective precipitation of the protein.

Thus, 0.3 M NaCl was determined to be optimal for generating smaller, spherical Ago2 precipitates while maintaining high precipitation efficiency.

3.1.2. Encapsulation of Ago2 nanoprecipitates into NPs and NP characterization

After obtaining the Ago2 protein nanoprecipitate, it was encapsulated into NPs made of PLGA-COOR/PLGA-PEG polymers to enhance Ago2 potential as a natural vector for RNAi delivery. The NPs were prepared using a phase separation method described in the literature to encapsulate proteins [36]. The PLGA derivatives were selected due to their biocompatibility, biodegradability, and proven effectiveness in

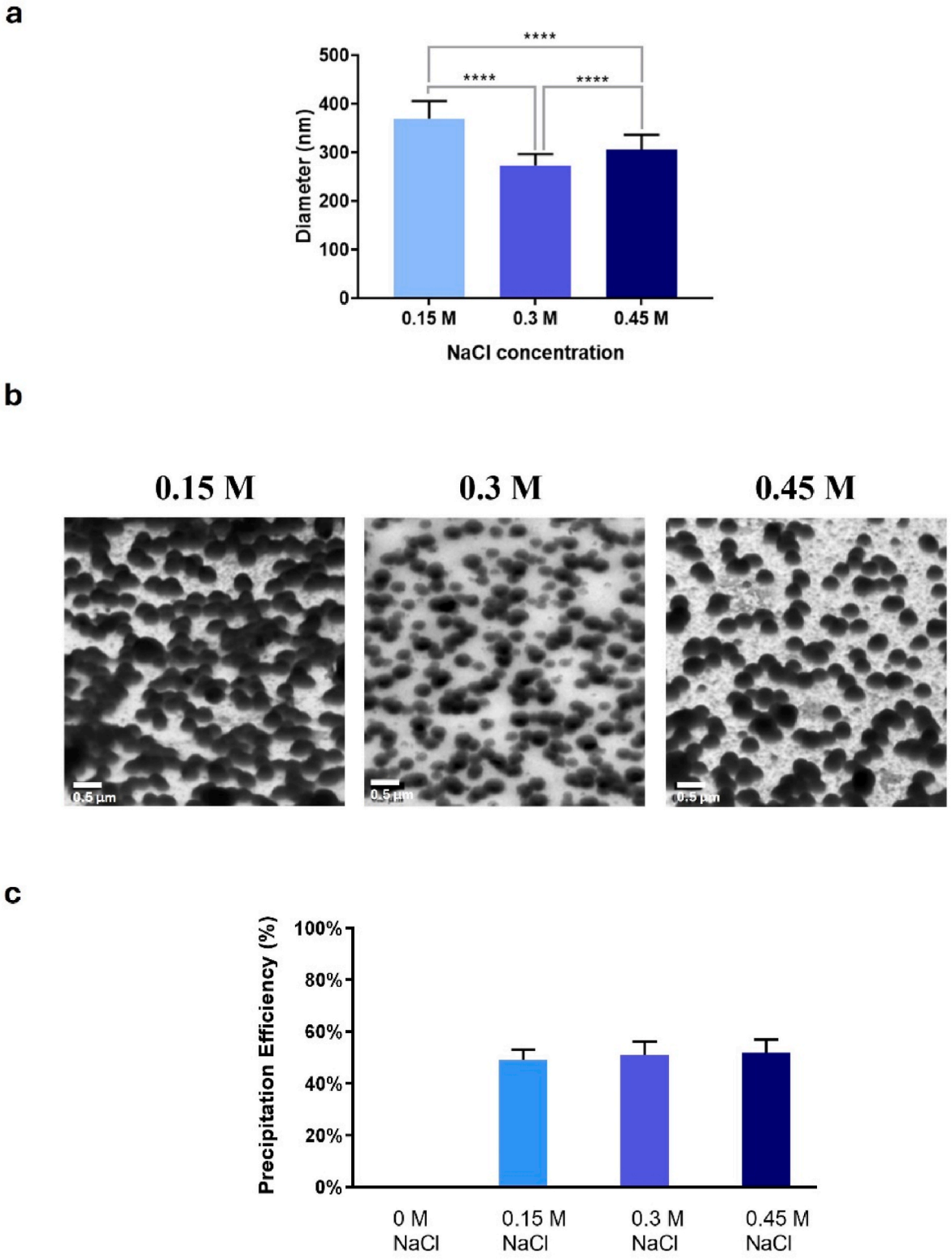

Fig. 1. Characterization of Ago2 nanoprecipitates depending on the NaCl concentration as a formulation condition. a) Diameter of Ago2 nanoprecipitates observed on TEM at different NaCl concentrations (0.15, 0.3, and 0.45 M) used to precipitate siAgo2 complexes, and b) corresponding TEM images of Ago2 precipitates acquired by using a sloping plane. Diameter values were measured using ImageJ software. All measurements were performed on a minimum of 50 nanoprecipitates (n = 50); c) effect of NaCl concentration on Ago2 precipitation efficiency. Statistical analysis was conducted to investigate any significant difference between samples prepared at 0.15 M, 0.3 M, and 0.45 M NaCl (n = 3 for each precipitation condition). Unpaired t-tests with Welch's correction were performed between each condition using GraphPad Prism 7.00 (****: $p < 0.0001$)—scale bars of TEM images: 0.5 µm. The absence of statistical signs indicates that no statistical difference was observed between graph bars.

a

	Ago2-loaded NPs (Ago2 NPs)			Blank NPs (F4)
Ago2 precipitates at	0.15 M NaCl (F1)	0.3 M NaCl (F2)	0.45 M NaCl (F3)	
Diameter (nm)	494±65 nm	312±48 nm	343±26 nm	206±4 nm
PDI	0.39±0.06	0.21±0.04	0.27±0.03	0.17±0.04
Zeta-Potential (mV)	-3.2±0.1	-2.4±0.2	-3.4±0.3	-2.3±0.3

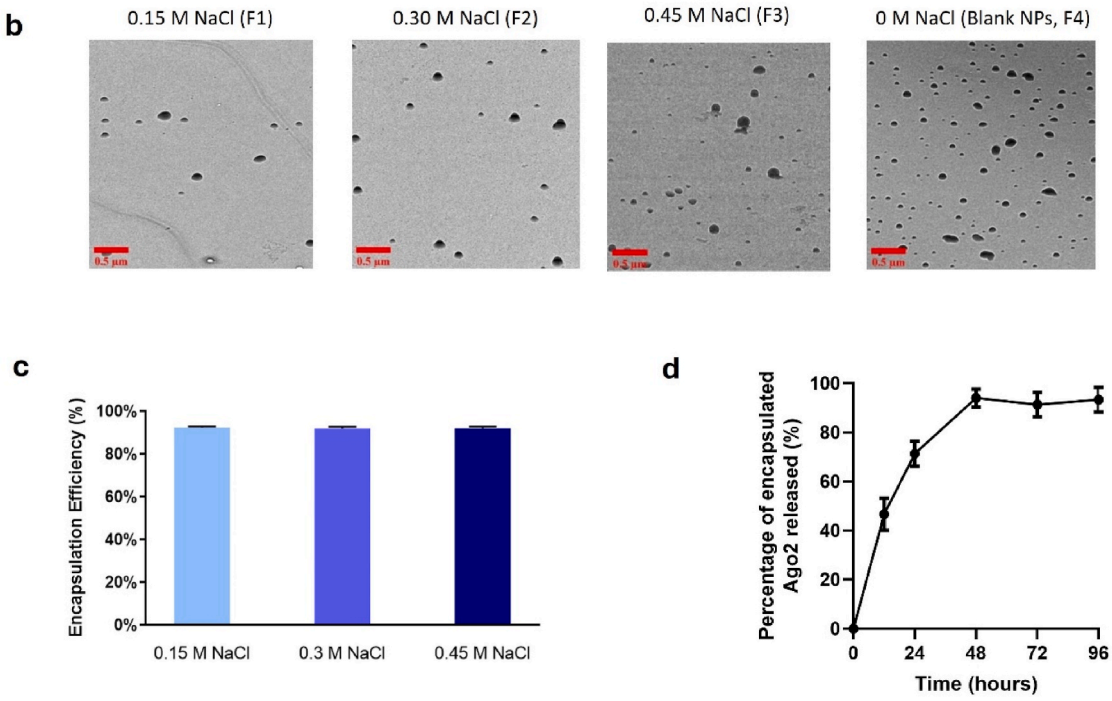

Fig. 2. Characterization of Ago2-loaded NPs depending on the NaCl concentration used to prepare the encapsulated Ago2 nanoprecipitates. a) Size (measured by DLS technique), PDI, Zeta-potential and c) Ago2 encapsulation efficiency of NPs loading Ago2 precipitates prepared using the aforementioned NaCl salt concentrations:0.15 M (F1), 0.3 M, (F2), and 0.45 M (F3) NaCl). Blank NPs (F4), used as a control, were formulated by replacing Ago2 with glycofurol solvent. b) TEM images of Ago2-loaded (F1-F3) or blank (F4) PLGA NPs depending on the Ago2 precipitate salt concentration; In b), since no nanoprecipitates were formed in the absence of salt, the control prepared at a 0 M NaCl concentration was not included. d) Release study of Ago2 NPs loading Ago2 nanoprecipitates formulated with 0.3 M NaCl concentration (optimized condition) in PBS buffer at pH 7.4. Data are given as mean ± SD.

protein encapsulation, as demonstrated in our previous studies [37].

Thus, the precipitated Ago2 was then encapsulated into NPs. To ensure that the NaCl molarity of the nanoprecipitates did not affect the Ago2 encapsulation into NPs, the three Ago2 precipitates, prepared using a different salt concentration of 0.15 M (F1), 0.3 M (F2), and 0.45 M (F3) NaCl, were encapsulated in the NPs. Then, the impact of this variable on NP characteristics was analyzed. Blank unloaded NPs (F4) were used as controls.

Dynamic Light Scattering (DLS) analyses yielded comparable mean diameters for F1-F4 formulations, being 494 ± 65 nm (F1), 328 ± 48 nm (F2), 343 ± 26 nm (F3), and 206 ± 4 nm (F4) (Fig. 2a). While the salt concentration used for precipitating Ago2 did not significantly affect NP size, the protein encapsulation notably increased NP sizes at all NaCl concentrations compared to the blank NPs (F4, Fig. 2a). This size difference was not observed in prior studies with SDF1-alpha protein, where precipitated protein was encapsulated under similar conditions [37]. This is likely due to the lower molecular weight of SDF1-alpha (8 kDa) compared to Ago2 protein (97 kDa), resulting in less polymer entanglement and smaller precipitates (<100 nm size). [37,46]. Moreover, the large size variability observed in TEM measurements, also observed in previous studies, may be due to the presence of a mixture in the sample of both empty and Ago2-loaded NPs [47]. The NPs also exhibited a PDI lower than 0.4, consistent with previous studies using this encapsulation method [36]. The Zeta-potential values of NPs ranged from −3.7 mV to −2.0 mV, nearly neutral (Fig. 2a). To ensure adequate colloidal stability, Zeta-potential values of less than −30 mV or more than +30 mV are typically considered optimal, as these values guarantee strong electrostatic repulsive interactions between NPs. However, concerns about their potential charge-related cytotoxicity have also been raised [48–51]. In this study, the inclusion of the exterior PEG layer and the end-capped PLGA in the nanosystem explained the almost neutral Zeta-potential observed for the developed NPs. Although the nanoparticle suspension lost electrostatic stability, it could benefit from the higher colloidal stability imparted by the steric repulsion given by PEG chains [52,53]. As shown in Fig. 2b, TEM images acquired by using a sloping plane confirmed the nanoparticle size observed by DLS analyses; they also showed that the NPs had a spherical morphology, despite a partial fusion of the NPs due to the drying step of the sample preparation and the heat of the beam of electrons. The Ago2 encapsulation efficiency (EE) of F1-F4 formulations for each salt concentration was also

determined. EE values for F1-F4 formulations were high (90–95 %) and reproducible, indicating successful formulation (Fig. 2c). Overall, both the Ago2 precipitation and encapsulation efficiencies were not affected by the salt concentration. Therefore, a single condition could be chosen for further studies. As previously mentioned, 0.3 M NaCl was chosen for the protein precipitation process, as this experimental condition led to the smallest sizes of both the precipitates and the NPs.

Finally, the release of Ago2 protein from Ago2-loaded NPs was investigated by suspending the NPs in a pH 7.4 PBS buffer solution at 37 °C and quantifying the Ago2 released from NPs at specific time intervals.

a

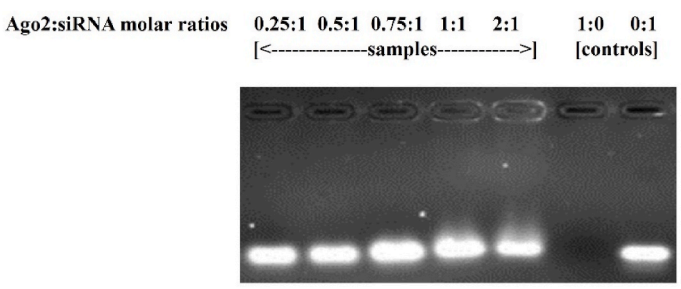

b

	Blank NPs	Ago2 NPs	siRNA/Ago2 NPs	siRNA NPs
Diameter (nm)	206 ± 4	312 ± 48	285 ± 56	214 ± 22
PDI	0.17 ± 0.08	0.21 ± 0.01	0.26 ± 0.06	0.24 ± 0.03
Zeta-Potential (mV)	-2.3 ± 0.3	-2.4 ± 0.2	-2.4 ± 0.2	-2.1 ± 0.4
Ago2 EE (%)	-	92.1 ± 2.3	85.1 ± 5.1	-
siRNA EE (%)	-	-	57.5 ± 11.4	7.3 ± 1.8

c

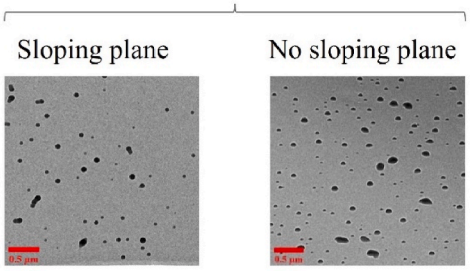

d

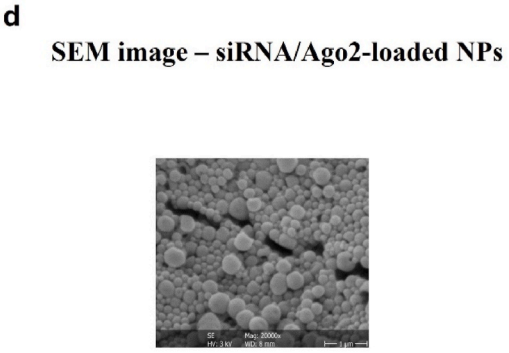

e

Cryoprotectant	Size (nm)		PDI		S_f/S_i	PDI_f/PDI_i
	Before freeze-drying	After Freeze-drying	Before freeze-drying	After Freeze-drying		
-	282 ± 29	n.d. [a]	0.24 ± 0.04	n.d. [a]	n.d. [a]	n.d. [a]
Trehalose		272 ± 18		0.20 ± 0.05	1.04	1.42
Sucrose		262± 84		0.60 ± 0.03	1.12	4.29

[a] n.d. = not determined as the freeze-dried product could not be reconstituted completely after 10 minutes sonication, and the measured size by DLS analyses was found to be > 1000 nm.

Fig. 3. Characterization of siRNA/Ago2 complexes and siRNA/Ago2 loaded NPs. **a**) Complexation of Ago2 with siRNA at different Ago2:siRNA molar ratios qualitatively assessed by Electrophoretic Mobility Shift Assays (EMSA). The control ratio 0:1 refers to siRNA alone in the absence of Ago2, while the ratio 1:0 refers to Ago2 not complexed with siRNA. **b**) Size, Polydispersity Index, Zeta-potential, and siRNA or Ago2 Encapsulation Efficiency (EE) of siRNA/Ago2 NPs versus Ago2 NPs and Blank NPs. Data are given as mean ± SD (n = 3). **c**) TEM Images of siRNA/Ago2 NPs acquired with (left) or without (right) the use on a sloping plane. Scale bar: 0.5 μm. **d**) SEM Images of siRNA/Ago2 NPs. Scale bar: 1 μm. **e**) Characterization of PLGA/PEG-PLGA NPs before and after freezing or freeze-drying with 5 % (w/w) HPBCD or sucrose as cryoprotectant. Frozen or freeze-dried NPs were re-suspended in 2 mL water and diluted to 100 μg/mL in before measurement. Data are presented as mean ± SD, n = 3.

The release profile revealed that approximately half of the encapsulated protein was released after 12 h (47 ± 8 %), followed by 71 ± 6 % release after 24 h, and 94 ± 3 % after 48 h (Fig. 2d). The initial burst release observed may be attributed to the leakage of the protein located near the surface of the NPs. The relatively short release duration aligns with findings from previous research [54,55]. However, a long-term purpose of this study is the integration of NPs into a hydrogel to be administered into the tumor resection cavity of GB patients after surgery, rather than direct suspension in physiological fluids. Extensive research indicates that the NP incorporation into the scaffold, if properly formulated, could prolong the protein release duration [56,57]. In our previous study, for instance, the integration of PLGA NPs containing the chemokine stromal cell-derived factor-1α (SDF-1α) into a chitosan-based electrospun nanofibrous scaffold extended release times up to five weeks, compared to free NPs that released the payload within three days [36].

3.2. Formation of siRNA/Ago2 complexes, precipitation, and encapsulation into NPs

After optimizing the precipitation and subsequent encapsulation of Ago2 alone into NPs, the optimal formulation conditions were used to prepare and characterize NPs loaded with siRNA/Ago2 complex. To this aim, the siRNA/Ago2 complex was first formed, followed by its encapsulation into NPs and the characterization of the siRNA/Ago2-loaded NPs.

First, an Electrophoretic Mobility Shift Assays (EMSA) was used to qualitatively assess the complexation of Ago2 with siRNA at different Ago2:siRNA molar ratios (ranging from 0:1 to 2:1), as well as to select the Ago2:siRNA molar ratio to use for encapsulation into NPs. This technique has been previously used by Seo et al. to detect Ago2-RNA interaction [58]. The complex formation was suggested by the observation of a shift of the siRNA band at the highest molar ratio tested (1:1) with respect to 0:1 ratio, corresponding to the migration of siRNA alone, and by the apparition of a band in the wells of the gel. This may be due to the formation of the complexes, which led to a retard in the migration of the bound siRNA (Fig. 3a). Higher Ago2:siRNA molar ratios could not be evaluated using this technique because the maximum loading capacity of each well in the electrophoresis gel was reached with the 2:1 M ratios. At the Ago2:siRNA ratio of 1:1, the presence of a residual band associated to free siRNA may suggest that this complexation is only partial. However, a hypothesis is that the complexation with siRNA, which may also occur at lower ratios, may alter the protein charge and consequently influence its migration along with siRNA. This is suggested by the staircase-like shift of the siRNA bands observed with increasing Ago2 ratios. As this technique enables to assess the complex formation only partially, it should be coupled with other techniques to validate its formation. However, a lack of adequate characterization of such complex is reported in the literature, mainly due to the difficulties related to inadequate sensitivity of most of the available techniques. The use of methods such as the Raman spectroscopy and the thermogravimetric analyses, for instance, are limited by the low amount of Ago2 protein used to formulate NPs or by the very high concentrations of siRNA and Ago2 protein necessary to perform the analysis, respectively. Moreover, in the case of Raman spectroscopy, the signals associated with the use of cryoprotectant by the manufacturer to lyophilize the protein, not specified but included in the composition, can obscure the signals associated with the protein itself [59,60]. However, previous studies report a biological effect of siRNA:Ago2 complex and an effective complex formation when a 1:1 Ago2:siRNA molar ratio is used [34,61,62]. By integrating the observation of our study with this evidence, the Ago2:siRNA 1:1 M ratio was selected for our studies.

Following the formation of the siRNA/Ago2 complex, Ago2 was precipitated using previously optimized experimental conditions (NaCl concentration: 3.0 M; stirring method: vortexing), and then encapsulated into PLGA-PEG and PLGA-COOR NPs. The siRNA/Ago2 NPs were characterized for morphology by TEM, size (by using both TEM and DLS analyses), polydispersity index, Zeta-potential, and both Ago2 and siRNA encapsulation efficiencies (EE). Ago2 NPs, blank NPs, and NPs loading siRNA without Ago2 (siRNA NPs) were used as controls. Although the size and EE of siRNA/Ago2 NPs were found to be lower than those of Ago2 NPs, this difference was not statistically significant (Fig. 3b). The variation in size may be attributed to the lower EE efficiency of Ago2, resulting in an increased proportion of empty NPs that failed to incorporate Ago2, thus resulting in a smaller size. The siRNA encapsulation efficiency was determined to be 57.5 ± 11.4 % for siRNA/Ago2 NPs and 7.3 ± 1.8 % for siRNA NPs, respectively (Fig. 3b). These results suggest the crucial role of Ago2 protein in enhancing the incorporation of Ago2 into PLGA NPs by acting as a pre-complexing agent. This is particularly relevant as the negative charges of PLGA are known to be a significant factor limiting the effective encapsulation of siRNA into NPs. Moreover, TEM and SEM images revealed that siRNA/Ago2 NPs exhibited a spherical shape (Fig. 3c and d).

Finally, the storage stability of siRNA/Ago2 NPs was evaluated. Polyesters, such as PLGA, are prone to degradation due to the hydrolysis of their ester bonds. This can cause the payload, encapsulated within polyester-based NPs, to leak out [63–65]. Our previous studies on NPs made up of PLGA-COOR/PLGA-PEG polymers have shown that the Zeta-potential of NPs became more negative over time in 0.05 M Tris-HCl buffer. This was attributed to the gradual hydrolysis of PLGA ester bonds, resulting in the exposure of negatively charged carboxylic acid terminals [37]. The use of a cryoprotectant to preserve the formulations from freeze-drying stresses is important to store them correctly [66,67]. In this study, hydroxypropyl cyclodextrin (HPBCD) and sucrose were used as cryoprotectants to assess their protective effect on freeze-dried formulations. The size and PDI of NPs before and after storage were measured after reconstitution under two conditions. NPs were considered stable throughout the freezing or freeze-drying process if the ratio of final to initial size (Sf/Si) and polydispersity index (PDIf/PDIi) was close to 1, where final and initial refer to parameters after and before storage, respectively [66]. Cryoprotectant-stabilized product could be fully reconstituted by sonication, and the size was preserved when using both HPBCD and sucrose, with Sf/Si ratios of 1.04 and 1.12, respectively. However, the PDIf/PDIi ratio was almost four times higher when using sucrose (4.29) than when using HBCD, indicating the superior ability of HPBCD to preserve the correct size distribution of NPs (Fig. 3e). Better results were obtained when using both cryoprotectants compared to the storage of NPs without cryoprotectants, which could not be resuspended completely even after 10-min sonication. This confirms the protective roles of these excipients. The superior protection ability of HBCD excipients may be explained by the experimental conditions used during the drying phase. During this step, the temperature should be kept below the collapse temperature (Tc) of the cryoprotectant to prevent the “collapse” of the freeze-dried products [68,69]. In this study, the minimal pressure and temperature that could be reached by the freeze-dryer used was 0.3 mbar and −20 °C, respectively. This temperature is below the Tc of HBCD, in the range between −15 °C and −30 °C [70], but not below the one of sucrose, whose Tc was found to be between −25 °C and −35 °C [71]. This may lead to higher residual humidity in the sample when using sucrose. Furthermore, the collapse of sucrose might induce a decrease in volume, narrowing the gap between the NPs, and thereby facilitating interactions among NP polymer chains and the formation of stable crystalline connections [72,73].

3.3. siRNA/Ago2 NPs as an effective and safe gene silencing system in GB cells

3.3.1. Luciferase gene silencing assay

To evaluate the ability of formulations to transfect siRNA into cancer cells and achieve efficient siRNA-mediated gene silencing *in vitro,* a luciferase gene reporter assay was used. Therefore, siRNA/Ago2 complexes were formulated using a siRNA targeting firefly luciferase mRNA

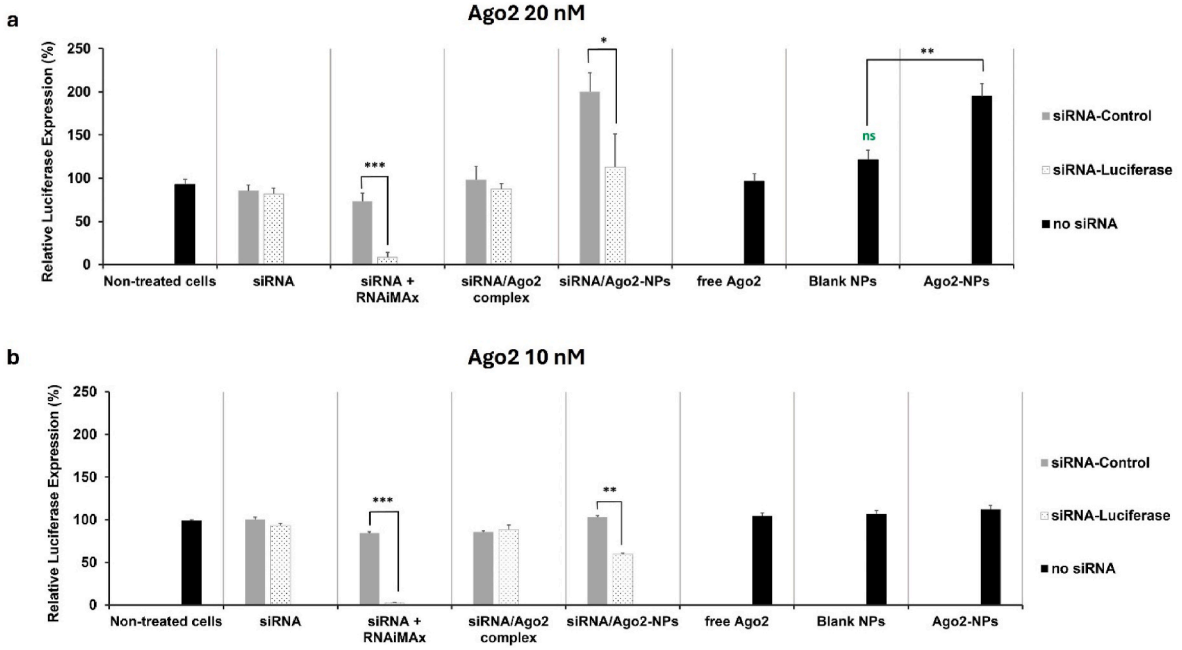

Fig. 4. Percentage of luciferase expression relative to non-treated cells in U87MG (Bmi1-3′UTR) cells 48 h after transfection with siRNA/Ago2 complexes delivering a siRNA-Luc (specific to luciferase) or siRNA-NC (non-targeting control), both free or encapsulated into NPs. Cells were incubated with Ago2 and siRNA/Ago2 complexes, both free or encapsulated into NPs, to achieve a final concentration of Ago2 per well of a) 20 nM or b) 10 nM. The final concentrations of siRNA were 20 nM and 10 nM, respectively, for the two concentrations of Ago2. NP concentration: 7.2 mg/mL. The final concentrations of siRNA were 20 nM and 10 nM, respectively, for the two concentrations of Ago2. siRNA/Ago2 complexes were prepared at an Ago2:siRNA molar ratio of 1:1. Data are given as the mean ± SD (*$p < 0.05$, **$p < 0.01$ and ***$p < 0.001$, one-way ANOVA and Post hoc analysis, $n = 3$. In a), the green symbol "ns" indicates no significant difference between the bar and non-treated cells.
siRNA-Luc = anti-luciferase siRNA; siRNA-NC = scramble negative control siRNA; BlankNPs = unloaded NPs; Ago2 NPs = NPs loaded with Ago2 only; free Ago2 and free siRNA = Ago2 and siRNA not loaded into NPs; RNAiMax™ = lipofectamine-based siRNA transfection agent.

sequence (siRNA-Luc). Luciferase gene silencing after 48-h transfection was evaluated *in vitro* on U87MG (Bmi1-3′UTR), a human GB cell model constitutively expressing the luciferase gene. Final concentration *in vitro* of 20 nM for siRNA and 20 nM for Ago2 was used. The gene silencing was evaluated by measuring the reduction in the Relative Luciferase Expression (RLE %) induced by each sample compared to an equivalent sample prepared using a siRNA negative control (siRNA-NC). Results were reported relative to viable cells and compared to non-treated cells. Blank NPs (unloaded), Ago2 NPs (without siRNA), free Ago2, and free siRNA were included as controls. Additionally, an industrial lipofectamine-based siRNA transfection agent (RNAiMax™) was used to verify the correct functionality of the assay. Results are shown in Fig. 4a.

When using the transfection agent RNAiMax™, the RLE with siRNA-Luc decreased significantly (from up to 8 ± 6 % compared to 73 ± 11 % using siRNA-NC), confirming the functionality of the test. As expected, free siRNA-Luc led to an RLE of about 100 %, confirming that naked siRNA-Luc itself cannot successfully silence the luciferase gene expression. However, no difference in the RLE between siRNA-Luc and siRNA-NC was observed even when delivering them as siRNA/Ago2 complexes. This suggests that siRNA/Ago2 *per se* was not an effective siRNA delivery system in the tested cell line and experimental conditions, despite the existence of literature describing Neuropilin-1 receptors, also expressed in U87MG cells, for Ago2 extracellular transport [74–76].

Leveraging Ago2's ability to stabilize siRNAs and form a minimal RISC-like complex *in vitro*, we sought to optimize its potential as a natural vector by incorporating it into NPs. Previous studies showed that polymeric NPs with a similar composition to the ones tested in this study could efficiently be internalized into U87MG cells [77,78]. Interestingly, the encapsulation of such complexes into siRNA/Ago2 NPs led to a significant downregulation of luciferase expression (115 ± 28 %) when carrying siRNA-Luc, compared to NPs formulated with the control siRNA (200 ± 34), confirming the effectiveness of such NP-based system in stabilizing the siRNA and induce a gene silencing effect.

In addition, an interesting effect could be observed in these experimental conditions (Fig. 4a): when Ago2 was incorporated into NPs, both in the presence of siRNA-NC (siRNA/Ago2 NPs) or in its absence (Ago2 NPs carrying Ago2 only), RLE values higher than 150 % were observed. This increase was also observed for NPs delivering siRNA-Luc, but the siRNA-mediated gene silencing effect reduced the RLE compared to the siRNA-NC-based counterparts. This effect was not statistically significant in the case of free Ago2 and blank NPs. Moreover, when cells were treated with NP formulations delivering half the dose of Ago2 (10 nM), the RLE did not exceed 110 % for any samples. This suggests that the rise in the RLE could be given the introduction of exogenous Ago2 into cells induced by the Ago2 NP-mediated uptake and in an Ago2 dose-dependent manner (Fig. 4b). Although recent evidence shows the effects of Ago2 overexpression into cells, it is not yet established whether the extrinsic administration of Ago2 leads to the same effects, due to differences in subcellular trafficking, distribution, and post-translational modifications. Our evidence raises the hypothesis that the delivery of exogenous Ago2 into GB cells could potentially stabilize RNAi molecules by facilitating the formation of a minimal RISC complex, and may also harness additional properties of Ago2 that extend beyond RNAi delivery [26,79]. These functions, likely not exclusive to RNAi-related processes, may involve interactions with the cellular machinery—both in the cytoplasm and possibly the nucleus, which remains to be fully explored

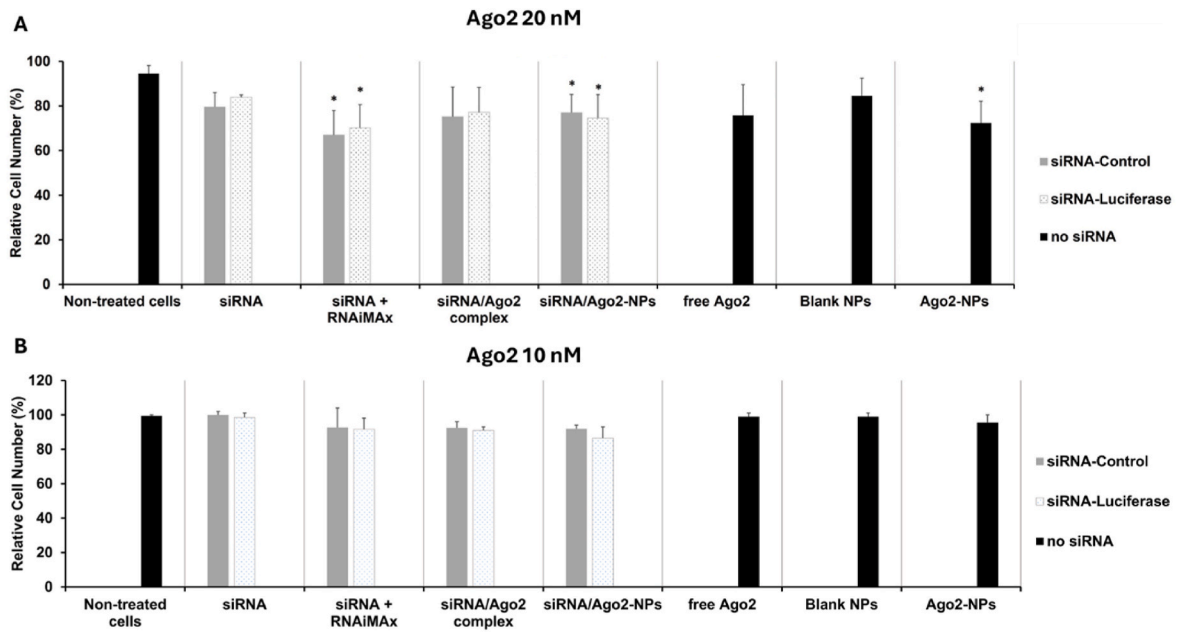

Fig. 5. Relative Cell Number obtained with a resazurin viability assay 48 h after U87MG (Bmi1-3′UTR) cell transfection with siRNA/Ago2 complexes delivering a siRNA-Luc (specific to luciferase) or siRNA-NC (non-targeting control), both free or encapsulated into NPs. Cells were incubated with Ago2 and siRNA/Ago2 complexes, both free or encapsulated into NPs, to achieve a final concentrations of Ago2 per well of a) 20 nM or b) 10 nM. The final concentrations of siRNA were 20 nM and 10 nM, respectively, for the two concentrations of Ago2. NP concentration: 7.2 mg/mL siRNA/Ago2 complexes were prepared at an Ago2:siRNA molar ratio of 1:1. Data are given as the mean ± SD (*$p < 0.05$, **$p < 0.01$ and ***$p < 0.001$, one-way ANOVA and Post hoc analysis, $n = 3$). Asterisks refer to significant statistical differences between each bar and the control bar of non-treated cells. The absence of asterisks in b) indicates no statistical difference between compared bars.
siRNA-Luc = anti-luciferase siRNA; siRNA-NC = scramble negative control siRNA; BlankNPs = unloaded NPs; Ago2 NPs = NPs loaded with Ago2 only; free Ago2 and free siRNA = Ago2 and siRNA not loaded into NPs; RNAiMax™ = lipofectamine-based siRNA transfection agent.

[80,81]. While our findings were not anticipated, they raise interesting questions that may inspire further research in this direction. Although still hypothetical at this stage, various studies in the literature echo the observation that Ago2 mays lift endogenous interference mechanisms that inhibit luciferase expression. For instance, studies have shown that Ago2 overexpression can enhance the cellular RNAi machinery, potentially altering miRNA availability [82,83]. Upon cellular uptake, exogenous Ago2 may interact with endogenous miRNAs that normally downregulate the luciferase gene expression. This interaction might alter the availability of these miRNAs to bind to target mRNA, thereby disrupting the normal miRNA-mediated gene silencing process [84]. Various mechanisms could be involved in this reduced miRNA availability, such as the squelching of endogenous miRNA or its Ago2-mediated differential compartmentalization, including sequestration within stress granules [85] or P-bodies (Processing bodies). P-bodies are cytoplasmic foci in various aspects of post-transcriptional gene regulation, including miRNA-mediated gene silencing, degradation of mRNAs that are faulty or no longer required for cell functions, or mRNA storage [86]. Studies have shown that a fraction of Ago2 in the cytoplasm can bind miRNAs and direct them to the P-bodies. Once within the P-body, the ribonucleoprotein system can target a specific mRNA for breakdown or keep it in a translationally repressed state for temporary storage [87,88]. To further explore the role of Ago2 in the RNAi regulatory machinery, future studies could replicate this experiment using the same cell line while targeting different gene expressions. A comprehensive transcriptomic analysis would help determine whether the observed overexpression phenomenon is a consistent outcome of Ago2 addition, either alone or in complex with siRNA. Such an approach would provide deeper insights into the mechanistic impact of Ago2 on gene regulation, reinforcing the significance of our findings and expanding our understanding of its broader functional implications. Given that siRNAs alone have no detectable biological effect, and that Ago2 is indeed present in the particles (cf. release profile and proper effect of vectorized Ago2), our *in vitro* observations indicate that siRNAs nanovectorized via Ago2 NPs exhibit biological activity. This suggests that siRNAs and Ago2 remain co-encapsulated within the nanocarrier during transfection. However, the precise subcellular trafficking of these two entities (Ago2 and siRNA) remains to be elucidated.

3.3.2. *Cancer cell viability*

The resazurin viability assay results are presented in Fig. 5. The cell viability is expressed in terms of Relative Cell Number (RCN) compared to non-treated cells. No difference in cell viability was observed after 48h cell transfection with free siRNA and free Ago2, while a modest but significant decrease in cell viability was observed for Ago2-containing NPs, both Ago2 NPs (74 ± 5) and siRNA/Ago2 NPs, in this last case with comparable results regardless of the use of control or luciferase siRNA (77 ± 8 for siRNA-NC and 75 ± 11 for siRNA-Luc) (Fig. 5a). Moreover, no significant decrease in cell viability was observed when using half of the NPs and Ago2 equivalent dose (Fig. 5b).

4. Concluding remarks and perspectives

This study introduces a novel delivery system based on the co-

delivery of siRNA and Ago2, a natural protein well known for its role in the RNAi machinery. As a pioneering approach, it exploits the documented ability of Ago2 to enhance the stability of RNAi molecules in cells, offering new opportunities for advancing siRNA delivery in RNAi-based therapies.

The system was tested both in its free form and encapsulated within NPs. After optimizing the Ago2 precipitation and encapsulation process, successful co-encapsulation of Ago2 and siRNA into the NPs was achieved. We found that Ago2 was crucial in promoting siRNA encapsulation into NPs.

Unlike free siRNA/Ago2 complexes, which were not effective for gene silencing on their own, the siRNA/Ago2-loaded NPs demonstrated significant gene silencing in a luciferase-expressing GB cell line. This suggests the potential of siRNA/Ago2 NPs as an efficient delivery system for GB cells, with potential application in local siRNA delivery strategies. Hence, future studies investigating the tissular and cellular fate of siRNAs from siRNA/Ago2-loaded NPs using *in vivo* nuclear imaging [92] or reporter systems [93] could provide valuable insights into their subcellular distribution, including their localization in cytoplasmic compartments relevant to RNA silencing such as GW or P-bodies [94]. In addition, this study envisions a long-term strategy where these NPs will be incorporated into a hydrogel scaffold for direct administration into the tumor resection cavity, enabling *in situ*and sustained siRNA availability within the brain. Further optimization of the formulation would be important to enhance the initial amount of Ago2 and siRNA, optimize the Ago2:polymer weight ratio, and minimize NP administration amounts.

Interestingly, we found that introducing exogenous Ago2 into cells via NPs produces effects beyond the expected RNAi delivery and gene silencing. These functions, likely not exclusive to RNAi-related processes, may involve interactions with the cellular machinery—both in the cytoplasm and possibly the nucleus. These findings encourage further investigation into the impact of exogenously introduced Ago2 on cells, particularly to explore whether its external administration elicits similar effects as endogenous overexpression, potentially influenced by differences in subcellular trafficking, distribution, and post-translational modifications.

Overall, this study represents a promising first step toward developing an innovative siRNA delivery system with potential therapeutic applications for locoregional GB treatment. Moreover, it lays the foundation for further exploration of the yet-undiscovered functional roles of exogenous Ago2 in cancer cells, extending beyond its currently known involvement in RNAi delivery.

CRediT authorship contribution statement

A. Rinaldi: Writing – original draft, Methodology, Investigation, Formal analysis. **E. Kluczka:** Methodology, Investigation, Formal analysis. **M. Louis Fathy Nazir:** Methodology, Investigation, Formal analysis. **M. Barbotin:** Formal analysis, Methodology, Visualization. **C. Roy:** Methodology, Investigation, Formal analysis. **L. Basset:** Methodology, Investigation, Formal analysis. **S. Avril:** Methodology, Investigation. **S. Anthiya:** Conceptualization. **G. Tosi:** Supervision, Resources. **C. Jérôme:** Resources, Conceptualization. **F. Boury:** Supervision, Funding acquisition. **A. Rousseau:** Validation, Supervision, Conceptualization. **E. Garcion:** Writing – original draft, Validation, Supervision, Project administration, Investigation, Funding acquisition, Formal analysis, Conceptualization. **F. Dumas:** Writing – original draft, Validation, Supervision, Conceptualization.

Declaration of competing interest

The authors declare that they have no known competing financial interests or personal relationships.

Acknowledgments

The work was supported by the Institut National de la Santé et de la Recherche Médicale (INSERM), the University of Angers, the Institut National du Cancer (INCa) under the frame of the PL-BIO project MARENGO, the “Ligue Nationale contre le Cancer” and the “Comité Départemental de Maine-et-Loire de la Ligue contre le Cancer” (CD49) under the frame of the FUSTARG project. It was additionally related to: the French National Agency for Research (ANR) under the frame of EuroNanoMed III (project GLIOSILK) [ANR-19-ENM3-0003-01]) and of the “France 2030 Investment Plan” Labex Iron [ANR-11-LABX-18- 01], the “Région Pays-de-la-Loire” under the frame of the TARGET’IN project and the “Tumour targeting, imaging and radio-therapies network” of the “Cancéropôle Grand-Ouest” (France). A. Rinaldi was a PhD fellow from the Program VINCI 2020 - Université Franco Italienne (project number: C3-1419, “Novel nanotechnological approaches for glioblastoma targeting”). Finally, the authors thank R. Mallet, R. Perrot and F. Manero from the SCIAM (Service Commun d’Imagerie et d’Analyses Microscopiques, Angers, France) for SEM and TEM analyses. We gratefully acknowledge that this publication contributed to a PhD thesis awarded the UFI 2025 Cotutelle PhD Prize by the Université Franco-Italienne. We thank the UFI for their support and kindly refer readers to their website https://www.universite-franco-italienne.org/fr/ for more information.

Appendix A. Supplementary data

Supplementary data to this article can be found online at https://doi.org/10.1016/j.jddst.2025.107459.

5. Appendix

A. Structures of PLGA, PLGA-PEG, and PLGA-COOR

Two types of polymers were used for the formulation of NPs, PEG-PLGA and R-PLGA. PLGA is a copolymer made up of glycolic and lactic acid monomers in a 50:50 ratio, which form aliphatic polyester (**A.1**). Its synthesis occurs through a ring-opening co-polymerization method of both glycolic and lactic acids, then monomeric units are linked by ester linkages. PEG-PLGA (MnPEG = 5 kDa, MnPLGA = 25.7 kDa) is an amphiphilic polymer whose structure is shown in **A.2**. R-PLGA (Mn = 5.5 kDa) is a PLGA with capped carboxylic acid terminals. Its carboxylic acid terminals are capped with an alkyl end-group, as shown in **A.3**.

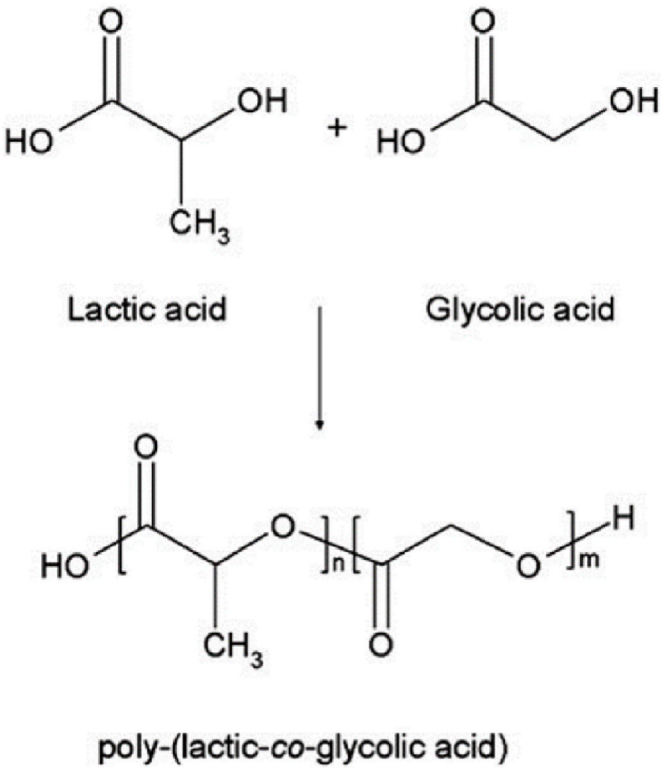

A.1: Poly-(D,L-Lactic-co-Glycolic) acid structure. Reproduced from Gentile et al., 2014 [89].

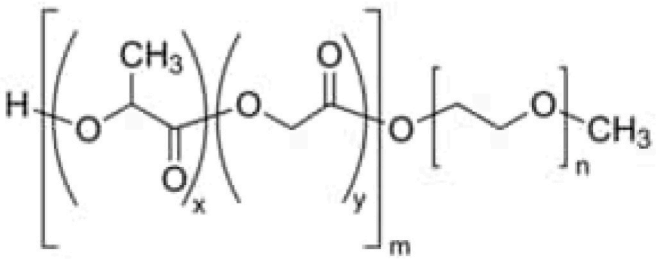

A.2: Poly Ethylene Glycol-Poly Lactic-co-Glycolic Acid structure. Reproduced from Sigma- Aldrich® [90].

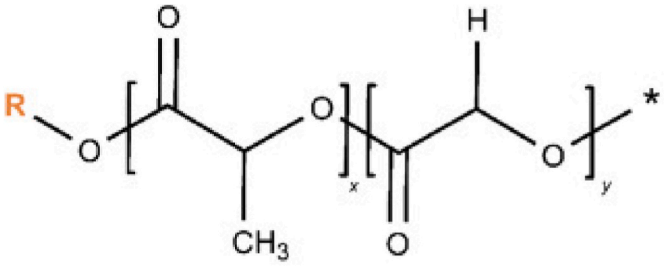

A.3: Poly Lactic-co-Glycolic Acid with capped carboxylic acid terminals structure. Where R represents an alkyl end group. Reproduced from Sequeira et al., 2020 [91].

B. siRNA-Luc sequence

The following information is about Firefly Luciferase siRNA, which is a custom design siRNA from Sigma®. It is a double-stranded RNA consisting of 42 nucleotides with two nucleotide overhangs. The molecular mass of the RNA is 12,722 g/mol. The sequence of the RNA from 5′ to 3′ is available in **B.1**. In Luciferase knockdown assays, MISSION® siRNA Universal Negative Control #1 (Sigma: SIC001) was used (sequence information not available).

CCGCAAGAUCCGCGAGAUU[dT][dT]: guide strand.

AAUCUCGCGGAUCUUGCGG[dT][dT]: passenger strand.

B.1: Luciferase siRNA sequence

Data availability

Data will be made available on request.

References

[1] C. Alifieris, D.T. Trafalis, Glioblastoma multiforme: pathogenesis and treatment, Pharmacol. Ther. 152 (2015) 63–82, https://doi.org/10.1016/j.pharmthera.2015.05.005.

[2] R.S. Angom, N.M.R. Nakka, S. Bhattacharya, Advances in glioblastoma therapy: an update on current approaches, Brain Sci. 13 (2023) 1536, https://doi.org/10.3390/brainsci13111536.

[3] R. Stupp, S. Taillibert, A. Kanner, W. Read, D.M. Steinberg, B. Lhermitte, S. Toms, A. Idbaih, M.S. Ahluwalia, K. Fink, et al., Effect of tumor-treating fields plus maintenance temozolomide vs maintenance temozolomide alone on survival in patients with glioblastoma: a randomized clinical trial, JAMA 318 (2017) 2306–2316, https://doi.org/10.1001/jama.2017.18718.

[4] E.K. Noch, R. Ramakrishna, R. Magge, Challenges in the treatment of glioblastoma: multisystem mechanisms of therapeutic resistance, World Neurosurg. 116 (2018) 505–517, https://doi.org/10.1016/j.wneu.2018.04.022.

[5] G.L. Liguori, Challenges and promise for glioblastoma treatment through extracellular vesicle inquiry, Cells 13 (2024) 336, https://doi.org/10.3390/cells13040336.

[6] C.V. Pecot, G.A. Calin, R.L. Coleman, G. Lopez-Berestein, A.K. Sood, RNA interference in the clinic: challenges and future directions, Nat. Rev. Cancer 11 (2011) 59–67, https://doi.org/10.1038/nrc2966.

[7] B. Hu, L. Zhong, Y. Weng, L. Peng, Y. Huang, Y. Zhao, X.-J. Liang, Therapeutic siRNA: state of the art, Signal Transduct. Targeted Ther. 5 (2020) 1–25, https://doi.org/10.1038/s41392-020-0207-x.

[8] S. Mirzaei, M.K. Mahabady, A. Zabolian, A. Abbaspour, P. Fallahzadeh, M. Noori, F. Hashemi, K. Hushmandi, S. Daneshi, A.P. Kumar, et al., Small interfering RNA (siRNA) to target genes and molecular pathways in glioblastoma therapy: current status with an emphasis on delivery systems, Life Sci. 275 (2021) 119368, https://doi.org/10.1016/j.lfs.2021.119368.

[9] M. Alghamdi, M. Gumbleton, B. Newland, Local delivery to malignant brain tumors: potential biomaterial-based therapeutic/adjuvant strategies, Biomater. Sci. 9 (2021) 6037–6051, https://doi.org/10.1039/D1BM00896J.

[10] A. Aigner, Gene silencing through RNA interference (RNAi) in vivo: strategies based on the direct application of siRNAs, J. Biotechnol. 124 (2006) 12–25, https://doi.org/10.1016/j.jbiotec.2005.12.003.

[11] S. Ashique, B. Almohaywi, N. Haider, S. Yasmin, A. Hussain, N. Mishra, A. Garg, siRNA-Based nanocarriers for targeted drug delivery to control breast cancer, Adv. Cancer Biol. - Meta. 4 (2022) 100047, https://doi.org/10.1016/j.adcanc.2022.100047.

[12] S. Colombo, D. Cun, K. Remaut, M. Bunker, J. Zhang, B. Martin-Bertelsen, A. Yaghmur, K. Braeckmans, H.M. Nielsen, C. Foged, Mechanistic profiling of the siRNA delivery dynamics of lipid-polymer hybrid nanoparticles, J. Contr. Release 201 (2015) 22–31, https://doi.org/10.1016/j.jconrel.2014.12.026.

[13] R. Bholakant, H. Qian, J. Zhang, X. Huang, D. Huang, J. Feijen, Y. Zhong, W. Chen, Recent advances of polycationic siRNA vectors for cancer therapy, Biomacromolecules (2020), https://doi.org/10.1021/acs.biomac.0c00438.

[14] L. Tang, R. Zhang, Y. Wang, X. Zhang, Y. Yang, B. Zhao, L.A. Yang, Simple self-assembly nanomicelle based on brain tumor-targeting peptide-mediated siRNA delivery for glioma immunotherapy via intranasal administration, Acta Biomater. 155 (2023) 521–537, https://doi.org/10.1016/j.actbio.2022.11.013.

[15] D.C. Arruda, A.-M. Lachagès, H. Demory, G. Escriou, R. Lai-Kuen, P.-Y. Dugas, C. Hoffmann, S. Bessoles, G. Sarrabayrouse, A. Malachias, et al., Spheroplexes: hybrid PLGA-cationic lipid nanoparticles, for in vitro and oral delivery of siRNA, J. Contr. Release 350 (2022) 228–243, https://doi.org/10.1016/j.jconrel.2022.08.030.

[16] J. Kim, J.Y. Kim, H. Kim, E. Kim, S. Park, K.-H. Ryu, E.G. Lee, Increasing transfection efficiency of lipoplexes by modulating complexation solution for transient gene expression, Int. J. Mol. Sci. 22 (2021) 12344, https://doi.org/10.3390/ijms222212344.

[17] T. Leite Nascimento, H. Hillaireau, J. Vergnaud, M. Rivano, C. Deloménie, D. Courilleau, S. Arpicco, J.S. Suk, J. Hanes, E. Fattal, Hyaluronic acid-conjugated lipoplexes for targeted delivery of siRNA in a murine metastatic lung cancer model, Int. J. Pharm. 514 (2016) 103–111, https://doi.org/10.1016/j.ijpharm.2016.06.125.

[18] M. Tang, Y. Hattori, Effect of using amino acids in the freeze-drying of siRNA lipoplexes on gene knockdown in cells after reverse transfection, Biomed. Rep. 15 (2021) 72, https://doi.org/10.3892/br.2021.1448.

[19] Y. Patil, J. Panyam, Polymeric nanoparticles for siRNA delivery and gene silencing, Int. J. Pharm. 367 (2009) 195–203, https://doi.org/10.1016/j.ijpharm.2008.09.039.

[20] H. Li, W. Lv, Y. Zhang, Q. Feng, H. Wu, C. Su, H. Shu, F. Nie, PLGA-PEI nanobubbles carrying PDLIM5 siRNA inhibit EGFR-TKI-Resistant NSCLC cell migration and invasion ability using UTND technology, J. Drug Deliv. Sci. Technol. 82 (2023) 104346, https://doi.org/10.1016/j.jddst.2023.104346.

[21] B.D. Monnery, M. Wright, R. Cavill, R. Hoogenboom, S. Shaunak, J.H.G. Steinke, M. Thanou, Cytotoxicity of polycations: relationship of molecular weight and the hydrolytic theory of the mechanism of toxicity, Int. J. Pharm. 521 (2017) 249–258, https://doi.org/10.1016/j.ijpharm.2017.02.048.

[22] W. He, X. Li, M. Morsch, M. Ismail, Y. Liu, F.U. Rehman, D. Zhang, Y. Wang, M. Zheng, R. Chung, et al., Brain-targeted codelivery of Bcl-2/Bcl-Xl and Mcl-1 inhibitors by biomimetic nanoparticles for orthotopic glioblastoma therapy, ACS Nano 16 (2022) 6293–6308, https://doi.org/10.1021/acsnano.2c00320.

[23] T. Wang, H. Zhang, W. Qiu, Y. Han, H. Liu, Z. Li, Biomimetic nanoparticles directly remodel immunosuppressive microenvironment for boosting glioblastoma immunotherapy, Bioact. Mater. 16 (2022) 418–432, https://doi.org/10.1016/j.bioactmat.2021.12.029.

[24] K.G. Gareev, D.S. Grouzdev, V.V. Koziaeva, N.O. Sitkov, H. Gao, T.M. Zimina, M. Shevtsov, Biomimetic nanomaterials: diversity, technology, and biomedical applications, Nanomaterials (Basel) 12 (2022) 2485, https://doi.org/10.3390/nano12142485.

[25] T.A. Rand, S. Petersen, F. Du, X. Wang, Argonaute2 cleaves the anti-guide strand of siRNA during RISC activation, Cell 123 (2005) 621–629, https://doi.org/10.1016/j.cell.2005.10.020.

[26] F.V. Rivas, N.H. Tolia, J.-J. Song, J.P. Aragon, J. Liu, G.J. Hannon, L. Joshua-Tor, Purified Argonaute2 and an siRNA form recombinant human RISC, Nat. Struct. Mol. Biol. 12 (2005) 340–349, https://doi.org/10.1038/nsmb918.

[27] E. Elkayam, C.-D. Kuhn, A. Tocilj, A.D. Haase, E.M. Greene, G.J. Hannon, L. Joshua-Tor, The structure of human Argonaute-2 in complex with miR-20a, Cell 150 (2012) 233, https://doi.org/10.1016/j.cell.2012.06.021.

[28] M.P. Hunter, N. Ismail, X. Zhang, B.D. Aguda, E.J. Lee, L. Yu, T. Xiao, J. Schafer, M.-L.T. Lee, T.D. Schmittgen, et al., Detection of microRNA expression in human peripheral blood microvesicles, PLoS One 3 (2008) e3694, https://doi.org/10.1371/journal.pone.0003694.

[29] K.C. Vickers, B.T. Palmisano, B.M. Shoucri, R.D. Shamburek, A.T. Remaley, MicroRNAs are transported in plasma and delivered to recipient cells by high-density lipoproteins, Nat. Cell Biol. 13 (2011) 423–433, https://doi.org/10.1038/ncb2210.

[30] S. Arroyo, M.J. Brodie, G. Avanzini, C. Baumgartner, C. Chiron, O. Dulac, J. A. French, J.M. Serratosa, Is refractory epilepsy preventable? Epilepsia 43 (2002) 437–444, https://doi.org/10.1046/j.1528-1157.2002.38501.x.

[31] J. Zhang, S. Li, L. Li, M. Li, C. Guo, J. Yao, S. Mi, Exosome and exosomal MicroRNA: trafficking, sorting, and function, Genom. Proteom. Bioinform. 13 (2015) 17–24, https://doi.org/10.1016/j.gpb.2015.02.001.

[32] Ferreira, R.; Santos, T.; Amar, A.; Gong, A.; Chen, T.C.; Tahara, S.M.; Giannotta, S. L.; Hofman, F.M. Argonaute-2 promotes miR-18a entry in human brain endothelial cells. J. Am. Heart Assoc. 3, e000968, doi:10.1161/JAHA.114.000968.

[33] G.J. Prud'homme, Y. Glinka, Z. Lichner, G.M. Yousef, Neuropilin-1 is a receptor for extracellular miRNA and AGO2/miRNA complexes and mediates the internalization of miRNAs that modulate cell function, Oncotarget 7 (2016) 68057–68071, https://doi.org/10.18632/oncotarget.10929.

[34] J. Li, C. Wu, W. Wang, Y. He, E. Elkayam, L. Joshua-Tor, P.T. Hammond, Structurally modulated codelivery of siRNA and argonaute 2 for enhanced RNA interference, Proc. Natl. Acad. Sci. 115 (2018) E2696–E2705, https://doi.org/10.1073/pnas.1719565115.

[35] D. Galas, R.E. Gelinas, C.B. Marsh, M.G. Piper, K. Wang, S. Zhang, METHODS, COMPOSITIONS, AND DEVICES UTILIZING Microrna TO DETERMINE PHYSIOLOGICAL CONDITIONS, 2010.

[36] R. Molina-Peña, M. Haji Mansor, M. Najberg, J.-M. Thomassin, B. Gueza, C. Alvarez-Lorenzo, E. Garcion, C. Jérôme, F. Boury, Nanoparticle-containing electrospun nanofibrous scaffolds for sustained release of SDF-1α, Int. J. Pharm. 610 (2021) 121205 https://doi.org/10.1016/j.ijpharm.2021.121205.

[37] M. Haji Mansor, M. Najberg, A. Contini, C. Alvarez-Lorenzo, E. Garcion, C. Jérôme, F. Boury, Development of a non-toxic and non-denaturing formulation process for encapsulation of SDF-1α into PLGA/PEG-PLGA nanoparticles to achieve sustained release, Eur. J. Pharm. Biopharm. 125 (2018) 38–50, https://doi.org/10.1016/j.ejpb.2017.12.020.

[38] A. Giteau, M.-C. Venier-Julienne, S. Marchal, J.-L. Courthaudon, M. Sergent, C. Montero-Menei, J.-M. Verdier, J.-P. Benoit, Reversible protein precipitation to ensure stability during encapsulation within PLGA microspheres, Eur. J. Pharm. Biopharm. 70 (2008) 127–136, https://doi.org/10.1016/j.ejpb.2008.03.006.

[39] R.L. McCall, R.W. Sirianni, PLGA nanoparticles formed by Single- or double-emulsion with vitamin E-TPGS, J. Vis. Exp. (2013) 51015, https://doi.org/10.3791/51015.

[40] L. Wang, P. Wang, Y. Liu, M.A. Mustafa Mahayyudin, R. Li, W. Zhang, Y. Zhan, Z. Li, The effect of different factors on Poly(Lactic-Co-Glycolic acid) nanoparticle properties and drug release behaviors when Co-Loaded with hydrophilic and hydrophobic drugs, Polymers 16 (2024) 865, https://doi.org/10.3390/polym16070865.

[41] A. Rinaldi, F. Dumas, J.T. Duskey, C. Imbriano, S. Belluti, C. Roy, I. Ottonelli, M. A. Vandelli, B. Ruozi, E. Garcion, et al., Polymer-lipid hybrid nanomedicines to deliver siRNA in and against glioblastoma cells, Int. J. Pharm. (2024) 123994, https://doi.org/10.1016/j.ijpharm.2024.123994.

[42] A. Giteau, M.-C. Venier-Julienne, S. Marchal, J.-L. Courthaudon, M. Sergent, C. Montero-Menei, J.-M. Verdier, J.-P. Benoit, Reversible protein precipitation to ensure stability during encapsulation within PLGA microspheres, Eur. J. Pharm. Biopharm. 70 (2008) 127–136, https://doi.org/10.1016/j.ejpb.2008.03.006.

[43] M. Andreev, V.M. Prabhu, J.F. Douglas, M. Tirrell, J.J. de Pablo, Complex coacervation in polyelectrolytes from a coarse-grained model, ACS Macro Lett. 51 (2018), https://doi.org/10.1021/acs.macromol.8b00556.

[44] C. Palocci, A. Valletta, L. Chronopoulou, L. Donati, M. Bramosanti, E. Brasili, B. Baldan, G. Pasqua, Endocytic pathways involved in PLGA nanoparticle uptake by grapevine cells and role of cell wall and membrane in size selection, Plant Cell Rep. 36 (2017) 1917–1928, https://doi.org/10.1007/s00299-017-2206-0.

[45] L. Mo, L. Hou, D. Guo, X. Xiao, P. Mao, X. Yang, Preparation and characterization of teniposide PLGA nanoparticles and their uptake in human glioblastoma U87MG cells, Int. J. Pharm. 436 (2012) 815–824, https://doi.org/10.1016/j.ijpharm.2012.07.050.
[46] W.-T. Choi, J. An, Biology and clinical relevance of chemokines and chemokine receptors CXCR4 and CCR5 in human diseases, Exp. Biol. Med. (Maywood) 236 (2011) 637–647, https://doi.org/10.1258/ebm.2011.010389.
[47] L.P. Dutta, M. Das, Coacervation—A method for drug delivery, in: S. Gupta, S. Bag, K. Ganguly, I. Sarkar, P. Biswas (Eds.), Proceedings of the Advancements of Medical Electronics, Springer India, New Delhi, 2015, pp. 379–386.
[48] S. Honary, F. Zahir, Effect of zeta potential on the properties of nano-drug delivery systems - a review (part 2), Trop. J. Pharmaceut. Res. 12 (2013), https://doi.org/10.4314/tjpr.v12i2.20.
[49] R. Kedmi, N. Ben-Arie, D. Peer, The systemic toxicity of positively charged lipid nanoparticles and the role of toll-like receptor 4 in immune activation, Biomaterials 31 (2010) 6867–6875, https://doi.org/10.1016/j.biomaterials.2010.05.027.
[50] E. Fröhlich, The role of surface charge in cellular uptake and cytotoxicity of medical nanoparticles, Int. J. Nanomed. 7 (2012) 5577–5591, https://doi.org/10.2147/IJN.S36111.
[51] C.R. Dass, Cytotoxicity issues pertinent to lipoplex-mediated gene therapy in-Vivo, J. Pharm. Pharmacol. 54 (2002) 593–601, https://doi.org/10.1211/0022357021778817.
[52] M.R. Mohammadi, A.V. Malkovskiy, P. Jothimuthu, K.-M. Kim, M. Parekh, M. Inayathullah, Y. Zhuge, J. Rajadas, PEG/dextran double layer influences Fe ion release and colloidal stability of iron oxide nanoparticles, Sci. Rep. 8 (2018) 4286, https://doi.org/10.1038/s41598-018-22644-8.
[53] L. Shi, J. Zhang, M. Zhao, S. Tang, X. Cheng, W. Zhang, W. Li, X. Liu, H. Peng, Q. Wang, Effects of polyethylene glycol on the surface of nanoparticles for targeted drug delivery, Nanoscale 13 (2021) 10748–10764, https://doi.org/10.1039/D1NR02065J.
[54] B. Devrim, A. Kara, İ. Vural, A. Bozkır, Lysozyme-loaded lipid-polymer hybrid nanoparticles: preparation, characterization and colloidal stability evaluation, Drug Dev. Ind. Pharm. 42 (2016) 1865–1876, https://doi.org/10.1080/03639045.2016.1180392.
[55] L. Huang, S. Wang, Z. Yin, Study in the stabilization of proteins encapsulated in PLGA delivery system: effects of additives on protein encapsulation, release, and stability, J. Drug Deliv. Sci. Technol. 73 (2022) 103436, https://doi.org/10.1016/j.jddst.2022.103436.
[56] S.Y. Chew, J. Wen, E.K.F. Yim, K.W. Leong, Sustained release of proteins from electrospun biodegradable fibers, Biomacromolecules 6 (2005) 2017–2024, https://doi.org/10.1021/bm0501149.
[57] R.M. Gebreel, N.A. Edris, H.M. Elmofty, M.I. Tadros, M.A. El-Nabarawi, D. H. Hassan, Development and characterization of PLGA nanoparticle-laden hydrogels for sustained ocular delivery of Norfloxacin in the treatment of pseudomonas Keratitis: an experimental study, DDDT 15 (2021) 399–418, https://doi.org/10.2147/DDDT.S293127.
[58] M. Seo, L. Lei, M. Egli, Label-free electrophoretic mobility shift assay (EMSA) for measuring dissociation constants of Protein-RNA complexes, Curr. Protoc. Nucleic Acid Chem. 76 (2019) e70, https://doi.org/10.1002/cpnc.70.
[59] S. Nasir, M.I. Majeed, H. Nawaz, N. Rashid, S. Ali, S. Farooq, M. Kashif, S. Rafiq, S. Bano, M.N. Ashraf, et al., Surface enhanced raman spectroscopy of RNA samples extracted from blood of hepatitis C patients for quantification of viral loads, Photodiagnosis Photodyn. Ther. 33 (2021) 102152, https://doi.org/10.1016/j.pdpdt.2020.102152.
[60] M. Almaghrabi, A. Alqurshi, S.A. Jadhav, F. Mazzacuva, A. Cilibrizzi, B. Raimi-Abraham, P.G. Royall, Evaluating thermogravimetric analysis for the measurement of drug loading in mesoporous silica nanoparticles (MSNs), Thermochim. Acta 730 (2023) 179616, https://doi.org/10.1016/j.tca.2023.179616.
[61] C.L. Noland, J.A. Doudna, Multiple sensors ensure guide strand selection in human RNAi pathways, RNA 19 (2013) 639–648, https://doi.org/10.1261/rna.037424.112.
[62] J. Je, P.T. Hammond, Y. He, W. Wang, Argonaute Protein-Double Stranded Rna Complexes and Uses Related Thereto, 2018.
[63] P. Fonte, S. Soares, A. Costa, J.C. Andrade, V. Seabra, S. Reis, B. Sarmento, Effect of cryoprotectants on the porosity and stability of insulin-loaded PLGA nanoparticles after freeze-drying, Biomatter 2 (2012) 329–339, https://doi.org/10.4161/biom.23246.
[64] J. Li, P. Nemes, J. Guo, Mapping intermediate degradation products of Poly(Lactic-Co-Glycolic acid) in vitro, J. Biomed. Mater. Res. B Appl. Biomater. 106 (2018) 1129–1137, https://doi.org/10.1002/jbm.b.33920.
[65] G. Longobardi, T.L. Moore, C. Conte, F. Ungaro, R. Satchi-Fainaro, F. Quaglia, Polyester nanoparticles delivering chemotherapeutics: learning from the past and looking to the future to enhance their clinical impact in tumor therapy, Wiley Interdiscip. Rev. Nanomed. Nanobiotechnol. 16 (2024) e1990, https://doi.org/10.1002/wnan.1990.
[66] M. Holzer, V. Vogel, W. Mäntele, D. Schwartz, W. Haase, K. Langer, Physico-chemical characterisation of PLGA nanoparticles after freeze-drying and storage, Eur. J. Pharm. Biopharm. 72 (2009) 428–437, https://doi.org/10.1016/j.ejpb.2009.02.002.
[67] P. Fonte, S. Reis, B. Sarmento, Facts and evidences on the lyophilization of polymeric nanoparticles for drug delivery, J. Contr. Release 225 (2016) 75–86, https://doi.org/10.1016/j.jconrel.2016.01.034.
[68] A. Merivaara, J. Zini, E. Koivunotko, S. Valkonen, O. Korhonen, F.M. Fernandes, M. Yliperttula, Preservation of biomaterials and cells by freeze-drying: Change of paradigm, J. Contr. Release 336 (2021) 480–498, https://doi.org/10.1016/j.jconrel.2021.06.042.
[69] G. Degobert, D. Aydin, Lyophilization of nanocapsules: instability sources, formulation and process parameters, Pharmaceutics 13 (2021) 1112. https://doi.org/10.3390/pharmaceutics13081112.
[70] M.C. Chamberlain, Temozolomide: therapeutic limitations in the treatment of adult high-grade gliomas, Expert Rev. Neurother. 10 (2010) 1537–1544, https://doi.org/10.1586/ern.10.32.
[71] J. Horn, W. Friess, Detection of collapse and crystallization of saccharide, protein, and mannitol formulations by optical fibers in lyophilization, Front. Chem. 6 (2018), https://doi.org/10.3389/fchem.2018.00004.
[72] G. Degobert, D. Aydin, Lyophilization of nanocapsules: instability sources, formulation and process parameters, Pharmaceutics 13 (2021) 1112, https://doi.org/10.3390/pharmaceutics13081112.
[73] F. De Jaeghere, E. Allémann, J.-C. Leroux, W. Stevels, J. Feijen, E. Doelker, R. Gurny, Formulation and lyoprotection of Poly(Lactic acid-co-ethylene oxide) nanoparticles: influence on physical stability and in vitro cell uptake, Pharm. Res. 16 (1999) 859–866, https://doi.org/10.1023/A:1018826103261.
[74] Z. Zou, Q. Lin, H. Yang, Z. Liu, S. Zheng, Nrp-1 mediated plasmatic Ago2 binding miR-21a-3p internalization: a novel mechanism for miR-21a-3p accumulation in renal tubular epithelial cells during sepsis, BioMed Res. Int. 2020 (2020) 2370253, https://doi.org/10.1155/2020/2370253.
[75] L. Chen, W. Miao, X. Tang, H. Zhang, S. Wang, F. Luo, J. Yan, The expression and significance of Neuropilin-1 (NRP-1) on glioma cell lines and glioma tissues, J. Biomed. Nanotechnol. 9 (2013) 559–563, https://doi.org/10.1166/jbn.2013.1624.
[76] B. Hu, P. Guo, I. Bar-Joseph, Y. Imanishi, M. Jarzynka, O. Bogler, T. Mikkelsen, T. Hirose, R. Nishikawa, S. Cheng, Neuropilin-1 promotes human glioma progression through potentiating the activity of the HGF/SF autocrine pathway, Oncogene 26 (2007) 5577–5586, https://doi.org/10.1038/sj.onc.1210348.
[77] Y. Kuang, S. An, Y. Guo, S. Huang, K. Shao, Y. Liu, J. Li, H. Ma, C. Jiang, T7 peptide-functionalized nanoparticles utilizing RNA interference for glioma dual targeting, Int. J. Pharm. 454 (2013) 11–20, https://doi.org/10.1016/j.ijpharm.2013.07.019.
[78] M. Malhotra, T.V. Sekar, J.S. Ananta, R. Devulapally, R. Afjei, H.A. Babikir, R. Paulmurugan, T.F. Massoud, Targeted nanoparticle delivery of therapeutic antisense microRNAs presensitizes glioblastoma cells to lower effective doses of temozolomide in vitro and in a mouse model, Oncotarget 9 (2018) 21478–21494, https://doi.org/10.18632/oncotarget.25135.
[79] I.J. MacRae, E. Ma, M. Zhou, C.V. Robinson, J.A. Doudna, In vitro reconstitution of the human RISC-loading complex, Proc. Natl. Acad. Sci. 105 (2008) 512–517, https://doi.org/10.1073/pnas.0710869105.
[80] Expanded RNA-binding activities of mammalian argonaute 2 | nucleic acids research, Oxford Academic Available online: https://academic.oup.com/nar/article/37/22/7533/2410050?login=true. (Accessed 14 February 2025).
[81] Full article: demystifying the nuclear function of argonaute proteins, Available online: https://www.tandfonline.com/doi/full/10.4161/rna.27604. (Accessed 14 February 2025).
[82] X. Zhang, P.R. Graves, Y. Zeng, Stable Argonaute2 overexpression differentially regulates microRNA production, Biochimica et Biophysica Acta (BBA) - Gene Regulat. Mech. 1789 (2009) 153–159, https://doi.org/10.1016/j.bbagrm.2008.11.004.
[83] K. Börner, D. Niopek, G. Cotugno, M. Kaldenbach, T. Pankert, J. Willemsen, X. Zhang, N. Schürmann, S. Mockenhaupt, A. Serva, et al., Robust RNAi enhancement via human Argonaute-2 overexpression from plasmids, viral vectors and cell lines, Nucleic Acids Res. 41 (2013) e199, https://doi.org/10.1093/nar/gkt836.
[84] F.V. Karginov, G.J. Hannon, Remodeling of Ago2-mRNA interactions upon cellular stress reflects miRNA complementarity and correlates with altered translation rates, Genes Dev. 27 (2013) 1624–1632, https://doi.org/10.1101/gad.215939.113.
[85] A. Detzer, C. Engel, W. Wünsche, G. Sczakiel, Cell stress is related to Re-Localization of argonaute 2 and to decreased RNA interference in human cells, Nucleic Acids Res. 39 (2011) 2727–2741, https://doi.org/10.1093/nar/gkq1216.
[86] A. Jakymiw, K.M. Pauley, S. Li, K. Ikeda, S. Lian, T. Eystathioy, M. Satoh, M. J. Fritzler, E.K.L. Chan, The role of GW/P-Bodies in RNA processing and silencing, J. Cell Sci. 120 (2007) 1317–1323, https://doi.org/10.1242/jcs.03429.
[87] A.K.L. Leung, P.A. Sharp, Quantifying argonaute proteins in and out of GW/P-Bodies: implications in microRNA activities, Adv. Exp. Med. Biol. 768 (2013) 165–182, https://doi.org/10.1007/978-1-4614-5107-5_10.
[88] J. Liu, M.A. Valencia-Sanchez, G.J. Hannon, R. Parker, MicroRNA-Dependent localization of targeted mRNAs to mammalian P-Bodies, Nat. Cell Biol. 7 (2005) 719–723, https://doi.org/10.1038/ncb1274.
[89] P. Gentile, V. Chiono, I. Carmagnola, P. Hatton, An overview of Poly(Lactic-Co-Glycolic) acid (PLGA)-based biomaterials for bone tissue engineering, IJMS 15 (2014) 3640–3659, https://doi.org/10.3390/ijms15033640.

[90] Poly(Ethylene glycol) methyl Ether-Block-Poly(Lactide-Co-Glycolide) - mpeg-b-plga, Available online: https://www.sigmaaldrich.com/FR/fr/substance/polyethyleneglycolmethyletherblockpolylactidecoglycolide1234598765. (Accessed 22 June 2022).
[91] J.A.D. Sequeira, I. Pereira, A.J. Ribeiro, F. Veiga, A.C. Santos, Chapter 8 - surface functionalization of PLGA nanoparticles for drug delivery. In *handbook of functionalized nanomaterials for industrial applications*, in: C. Mustansar Hussain (Ed.), Micro and Nano Technologies, Elsevier, 2020, pp. 185–203.
[92] H. Hong, Y. Zhang, W. Cai, In vivo imaging of RNA interference, J. Nucl. Med. 51 (2010) 169–172, https://doi.org/10.2967/jnumed.109.066878.
[93] V. Simion, C. Loussouarn, Y. Laurent, L. Roncali, D. Gosset, F. Reverchon, A. Rousseau, F. Martin, P. Midoux, C. Pichon, et al., LentiRILES, a miRNA-ON sensor system for monitoring the functionality of miRNA in cancer biology and therapy, RNA Biol. 18 (2021) 198–214, https://doi.org/10.1080/15476286.2021.1978202.
[94] A. Safieddine, M.N. Benassy, T. Bonte, F. Slimani, O. Pourcelot, M. Kress, M. Ernoult-Lange, M. Courel, E. Coleno, A. Imbert, et al., Cell-cycle-dependent mRNA localization in P-bodies, Mol Cell 84 (2024) 4191–4208 e4197, https://doi.org/10.1016/j.molcel.2024.09.011.